J. Membrane Biol. 86, 167–187 (1985)

The Journal of
Membrane Biology

A Minimum Mechanism for Na^+–Ca^{++} Exchange: Net and Unidirectional Ca^{++} Fluxes as Functions of Ion Composition and Membrane Potential

Edward A. Johnson and J. Mailen Kootsey
Department of Physiology, Duke University Medical Center, Durham, North Carolina 27710

Summary. Both simultaneous and consecutive mechanisms for Na^+–Ca^{++} exchange are formulated and the associated systems of steady-state equations are solved numerically, and the net and unidirectional Ca^{++} fluxes computed for a variety of ionic and electrical boundary conditions. A simultaneous mechanism is shown to be consistent with a broad range of experimental data from the squid giant axon, cardiac muscle and isolated sarcolemmal vesicles. In this mechanism, random binding of three Na^+ ions and one Ca^{++} on apposing sides of a membrane are required before a conformational change can occur, translocating the binding sites to the opposite sides of the membranes. A similar (return) translocation step is also permitted if all the sites are empty. None of the other states of binding can undergo such translocating conformational changes. The resulting reaction scheme has 22 reaction steps involving 16 ion-binding intermediates. The voltage dependence of the equilibrium constant for the overall reaction, required by the 3:1 Na^+:Ca^{++} stoichiometry was obtained by multiplying and dividing, respectively, the forward and reverse rate constants of one of the translocational steps by $\exp(-FV/2RT)$. With reasonable values for the membrane density of the enzyme ($\approx$120 sites μm^{-2}) and an upper limit for the rate constants of both translocational steps of $10^5 \cdot sec^{-1}$, satisfactory behavior was obtainable with identical binding constants for Ca^{++} on the two sides of the membrane (10^6 M^{-1}), similar symmetry also being assumed for the Na^+ binding constant (12 to 60 M^{-1}). Introduction of order into the ion-binding process eliminates behavior that is consistent with experimental findings.

Key Words sodium-calcium exchange · ion-binding · enzyme · reaction theory · unidirectional flux · stoichiometry

Introduction

Intracellular Ca^{++} plays a key role in the functioning of a wide variety of cells as a "second messenger," activating secretion, muscle contraction, the release of neurotransmitters in synaptic transmission, the opening of membrane ion channels, fertilization, . . . to name but a few. A knowledge of how the concentration of intracellular Ca^{++} is regulated is therefore essential for an understanding of a wide variety of physiological mechanisms. There appear to be two mechanisms in the plasmalemma of cells that act to maintain the free calcium ion concentration within cells some 4 to 5 orders of magnitude lower than that in extracellular space: (1) a Ca^{++}-ATPase pump driven by the free energy of splitting of adenosine triphosphate (ATP) and (2) an exchange molecule that transports Ca^{++} out of the cell by utilizing the electrochemical free energy of the transmembrane [Na^+] gradient—the Na^+–Ca^{++} exchanger. The latter mechanism, especially, has received extensive study in a wide variety of preparations, notably the squid giant axon, isolated plasmalemmal vesicles, and cardiac muscle, with the result that there is a rich literature describing its electrical and chemical dependences. Because of its dependence on the Na^+ gradient, the exchanger is in effect dependent on the activity of the plasmalemmal Na^+,K^+-ATPase, the Na^+,K^+ transport of which determines that gradient. The prime regulators of the rate of Na^+,K^+ transport, as well as that of Na^+–Ca^{++} exchange are the intra- and extracellular concentrations of the transported ion species themselves, i.e. Na^+,K^+ and Ca^{++}, together with the transmembrane potential (since both mechanisms are electrogenic). For this reason the regulation of each mechanism is interlocked with one another, since each transports a common ion species, namely Na^+. Furthermore, a prime modulator of Na^+–Ca^{++} exchange is the concentration of intracellular Ca^{++} itself, which in turn is regulated by other intracellular transport mechanisms (sarco/endoplasmic reticulum and mitochondrial transport) as well as the plasmalemmal ATP-driven Ca^{++} pump mentioned above.

The main purpose of the present paper was to formulate a minimum mechanism for Na^+–Ca^{++} exchange and demonstrate that its behavior was in qualitative accord, at least as a first approximation, with that observed experimentally in three widely used preparations, namely, squid giant axon, car-

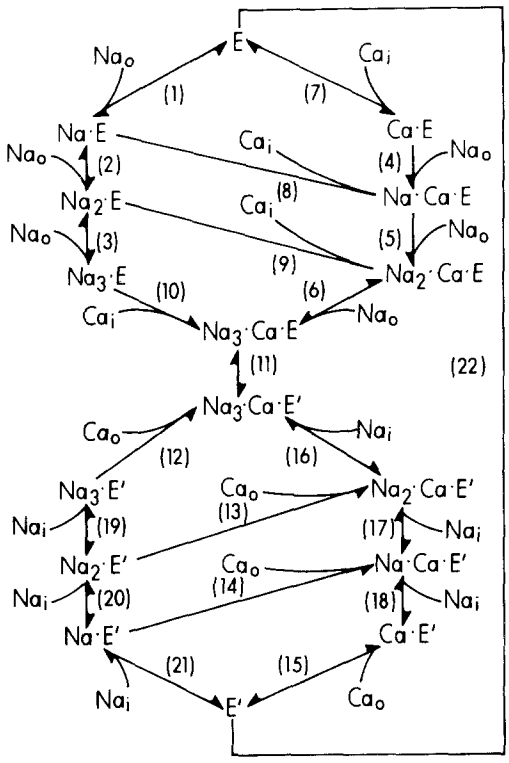

Fig. 1. Simultaneous mechanism for Na^+–Ca^{++} exchange with a stoichiometry of 3 Na^+ : 1 Ca^{++}. Either of the 2 translocational steps (11) and (22) were made voltage dependent by multiplying the forward and dividing the backward rate constants (as defined by the rate equations listed in Materials and Methods) for either of these steps by $\exp(-FV/2RT)$. If both steps were made voltage dependent, the forward and backward rate constants of both steps were multiplied and divided, respectively, by $\exp(-FV/4RT)$. In all cases the resultant effect was to render the equilibrium constant for the entire exchange process equal to $\exp(-FV/RT)$

diac sarcolemmal vesicles and intact cardiac muscle. In the process we hoped to illustrate some of the principles and properties that apply to exchange/transport processes in general. We were also interested in making, eventually, a comprehensive reconstruction of the cell system for the regulation of intracellular calcium based on present biochemical and physiological knowledge of the behavior of the various component mechanisms studied in relative isolation. To these ends we wanted to formulate a mechanism of Na^+–Ca^{++} exchange along the lines we have previously employed for the Na^+,K^+ pump (Chapman et al., 1983; Johnson & Chapman, 1984). Since we intended the behavior of such a mechanism to be consistent with a reasonably wide range of experimental observation, we saw the mechanism as also being useful as a guide in the design of strategic experiments to explore the nature of the actual mechanism of Na^+–Ca^{++} exchange, as well as aid in the interpretation of present and future experimental findings.

Mullins (1977) and Wong and Bassingthwaighte (1981) have proposed kinetic schemes for Na^+–Ca^{++} exchange, deriving algebraic equations relating the net ion fluxes to the model parameters. While this gave insight into the fundamental properties of exchange mechanisms, their schemes imposed an arbitrary order on the process of ion binding, most likely because of the need to keep the equations to manageable proportions. We were anxious from the outset to avoid such necessity since we wished to find the simplest mechanism consistent with experimental findings which, as will be shown, is one in which the ions bind randomly to independent sites on the exchanger. Indeed, the imposition of order on the ion-binding was found to destroy properties that were in keeping with experimental finding. In addition, since much of the experimental literature deals with isotopic ion fluxes, we have calculated the unidirectional as well as the net calcium fluxes. All of this was made feasible from a practical point of view by obtaining numerical rather than analytical solutions to the systems of steady-state equations.

Our conclusions concerning the general properties of the mechanistically simple exchangers that we have studied are much in accord with those of Sanders et al. (1984) concerning their generalized analysis of ion-drived cotransport systems. We found, as did they, that the mechanisms, free of mathematically simplifying assumptions, exhibit a richness and complexity of behavior that obviates the need, otherwise, to add mechanistic complexities in order to restore behavioral complexities that were lost in imposing the assumptions in the first place.

The Mechanism

Choice of Mechanism

Two kinds of mechanism for Na^+–Ca^{++} exchange were considered. In the first, the exchange of both ion species occurs *simultaneously* in one translocational step; both Na^+ and Ca^{++} bind randomly to the exchanger, n Na^+ on one side and 1 Ca^{++} on the other, followed by their translocation and release on opposite sides of the membrane. In the second, the exchange of Na^+ and Ca^{++} occurs *consecutively* in two separate translocational steps: in one step, either n Na^+ or 1 Ca^{++} bind on one side (A) and are then translocated to the other side (B) of the membrane; in the second step, the other ion species binds to side (B) to be translocated back to the origi-

nal side (A). In both schemes there are two translocational forms of the enzyme: in the consecutive mechanism translocational changes from one form to the other are always accompanied by the translocation of ions whereas in the simultaneous mechanism one translocational change must occur with all ion binding sites empty. These two kinds of mechanism are illustrated by the two schemes shown in Figs. 1 and 2.

Figure 1 shows a simultaneous mechanism in which 3 Na^+ and 1 Ca^{++} can bind randomly and reversibly to Na^+- and Ca^{++}-selective sites on opposite sides of the membrane. When, and only when, all binding sites are occupied, the enzyme undergoes a conformational change so that these same binding sites now face opposite sides of the membrane where the ions are free to associate and dissociate randomly. A second translocatable form of the enzyme exists in which all the binding sites are empty, the two forms cycling back and forth across the membrane thereby enabling net ion transport to occur.[1]

Figure 2 shows a consecutive mechanism which, although the simplest mechanistically, can be seen to be more ordered in ion binding than the simultaneous scheme of Fig. 1. One Ca^{++} binds intracellularly to the enzyme (step [1]), a conformational change then occurs (step [2]) which translocates the Ca^{++} to face the outside of the cell where it is free to dissociate (step [3]). In this second free state, E', the enzyme is able to bind three Na^+ in random fashion (steps [4] thru [6]). With all three Na^+ bound the enzyme undergoes a second conformational change (step 7) which translocates the ions to face the inside of the cell. There they are free to dissociate, one after the other, to restore the enzyme to its original free (E) form which binds Ca^{++} once more to cycle through the above sequence again.

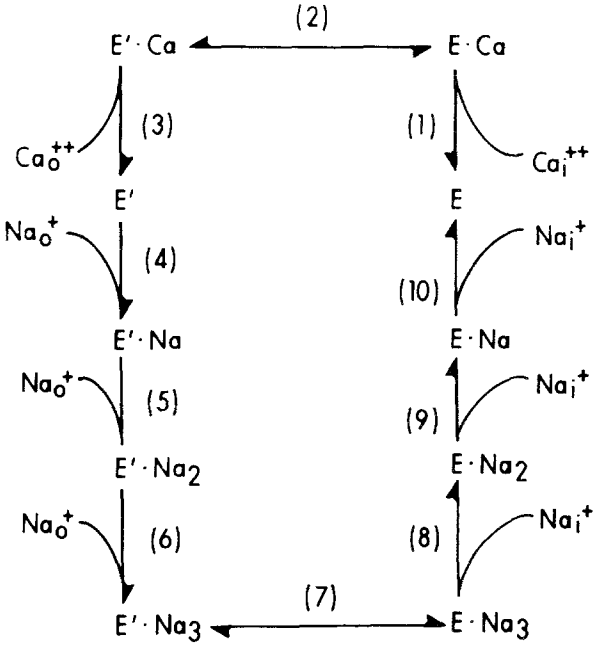

Fig. 2. Consecutive mechanism for Na^+–Ca^{++} exchange with a stoichiometry of 3 Na^+ : 1 Ca^{++}. Either of the 2 translocational steps (2) and (7) were made voltage dependent by multiplying the forward and dividing the backward rate constants (as defined by the rate equations listed in Materials and Methods) for either of these steps by $\exp(-FV/2RT)$. If both steps were made voltage dependent, the forward and backward rate constants of both steps were multiplied and divided, respectively, by $\exp(-FV/4RT)$. In all cases the resultant effect was to render the equilibrium constant for the entire exchange process equal to $\exp(-FV/RT)$

All steps in both schemes are reversible. The individual unidirectional forward and reverse rates for any given step are governed by the concentrations of the ion species and the particular forms of the enzyme associated with that step, together with the forward and reverse rate constants, f_n and b_n, respectively, for that step. In the absence of a transmembrane potential (*see* Voltage Dependence), the equilibrium constant of either mechanism, i.e., the ratio of the product of all forward rate constants to the product of all reverse rate constants of the elementary steps, must equal unity.

Although both simultaneous and consecutive mechanisms were studied, the simultaneous form will receive the most attention in this paper (*see* Results and Discussion). The prime reason for this bias is that a characteristic of the experimental observations regarding Na^+–Ca^{++} exchange is that relatively little, if any, Ca^{++}–Ca^{++} exchange occurs in the absence of Na^+. As will be discussed later, such exchange is inherent in consecutive mechanisms, whereas it appears inherently impossible in simultaneous mechanisms. As a consequence, con-

[1] A reduced form of the mechanism of Fig. 1, similar to that proposed by Mullins (1977), could have been studied that would have been much simpler to describe mathematically. Three Na^+ ions bind one after the other to the enzyme on one side of the membrane (equivalent to steps [1] thru [3] of Fig. 1) followed, on the other side, by one Ca^{++} ion (step [10]). With all binding sites occupied, a conformational change in the enzyme occurs (step [11]) which translocates the bound ions to face opposite sides of the membrane, where they are free to dissociate, first Ca^{++} in step [12] followed by the 3 Na^+ in steps [19] thru [21]. That is to say, a 7 state, 7 step mechanism. This scheme, however, presupposes considerable ordering in the ion binding. Indeed, an additional conformational change is implied by the restriction that Ca^{++} binds only when the 3 Na^+ are bound. The full scheme of Fig. 1, although mathematically more complex to describe, is mechanistically simpler. Moreover, as will be shown later the behavior of the reduced mechanism is markedly different in some respects from the fully randomized mechanism of Fig. 1.

secutive schemes were eliminated at the outset of our studies as possible candidates for a realistic mechanism of Na^+–Ca^{++} exchange. Indeed, investigators in the field have favored a simultaneous rather than a consecutive mechanism (Baker et al., 1969; Blaustein, 1977; Mullins, 1977; DiPolo, 1979; Wong & Bassingthwaighte, 1981; Ledvora & Hegyvary, 1983).

Stoichiometry

There now seems to be general agreement that for Na^+–Ca^{++} exchange to effect net transport of Ca^{++} out of the cell at the concentrations of Na^+ and Ca^{++} and membrane potentials found physiologically, the stoichiometric ratio of Na^+ to Ca^{++} transported must exceed 2. If the ratio is assumed to be an integral number, which is necessarily desirable for reasons of mechanistic simplicity, if not realistic probability, the evidence points to a ratio of 3. Certainly this is the case for cells for which the ion concentrations are known with reasonable certainty. In sheep ventricular muscle, $[Na^+]_o$, $[Na^+]_i$, $[Ca^{++}]_o$, and the resting potential had the following values (Sheu & Fozzard, 1982): 151.5 mM, 8.4 mM, 1.8 mM, and −90 mV at 34°C. With a stoichiometric ratio of 3, the equilibrium value for $[Ca^{++}]_i$, is 10.2 nM—far less than the observed values of close to 200 nM. The stoichiometric ratios calculated by Sheu and Fozzard (1982) from these and similar measurements, on the assumption that the exchanger was at or very close to equilibrium, were always greater than 2, indeed were found to be consistently around 2.5. This value of 2.5 is in keeping with an actual ratio of 3 if the exchanger were significantly away from equilibrium, which is not unreasonable given the often highly nonlinear relation between flux and driving force that we found with the mechanisms studied in the present paper. The ratio of net Na^+ loss to net Ca^{++} gain in rabbit ventricular muscle attributed to Na^+–Ca^{++} exchange was found to be 3.0 (Bridge & Bassingthwaighte, 1983), indicating a stoichiometric ratio of at least 3, which is in keeping with the ratio estimated by Pitts (1979) in cardiac sarcolemmal vesicles.

Although some authors (e.g., Mullins 1977) favor a stoichiometric ratio of 4 in the squid giant axon, the ion gradients and membrane potential in that tissue are nonetheless in keeping with a ratio of 3, as are direct measurements of stoichiometry (Blaustein & Russell, 1975). Taking the ionic concentrations listed by Requena (1983) for the squid giant axon ($[Na^+]_o = 461 \pm 28$ mM, $[Na^+]_i = 27 \pm 2$ mM, $[Ca^{++}]_o = 3 \pm 1$ mM) and again a stoichiometry ratio of 3, the equilibrium value for $[Ca^{++}]_i$, (20°C) in the *in vivo* axon with a resting potential of −70 mV is 37.7 nM, less than the observed value (*see below*). For the resting potential of −60 mV in the *in vitro* axon (Requena, 1983) it is 56 nM, which is not significantly different from the observed value cited by Requena (1983) of 0.05 ± 0.05 μM, and is well below the value of 100 nM reported by Baker (1976; recalculated from data of Baker et al., 1971) and 106 nM reported by DiPolo et al. (1983). Moreover, even were the equilibrium value somewhat greater than the observed value for $[Ca^{++}]_i$, this is still consistent with a steady state for intracellular $[Ca^{++}]$ since there is an additional Ca^{++} extrusion mechanism in the plasmalemma of squid axon (the "uncoupled pump"; Baker & McNaughton, 1978), the Ca^{++}-ATPase, with a $K_{0.5} \approx 0.2$ μM and a maximum efflux rate ≈ 200 fmol · cm^{-1} sec^{-1} (DiPolo & Beauge, 1979, 1980). Indeed, it appears that 85 to 90% of the Ca^{++} extrusion in the resting axon is via the ATP-driven Ca^{++} pump (*cf.* DiPolo & Beauge, 1983; their Table 2).

A stoichiometric ratio of 3 was therefore used in all the mechanisms studied.

Choice of Rate Constants

Ion-Binding Constants

Experimental evidence from the squid axon and especially cardiac sarcolemmal vesicles suggest that the ion-binding characteristics for each ion species on the two sides of the membrane are the same. DiPolo and Beauge (1980) stress the view that the exchanger is symmetrical in that the driving and driven ion species can exchange roles by suitable manipulation of their gradients, resulting in Na_i^+-dependent Ca^{++} influx, Ca_o^{++}-dependent Na^+ efflux, Na_o^+-dependent Ca^{++} efflux and Ca_i^{++}-dependent Na^+ influx. More specifically, Philipson and Nishimoto (1982) compared Na^+-dependent Ca^{++} uptake into inside-out vesicles with that into the total, primarily of right-side-out vesicles. They found no difference in the $K_M(Ca^{++})$, nor in the responses to altered pH or valinomycin-induced membrane potentials. Their findings are remarkable, considering the large difference in the Ca^{++} concentration on the two sides of the membrane found physiologically (factor of ≈ 10^4 to 10^5). We decided therefore that unless other experimental findings demanded otherwise, we would constrain our choices of rate constants to make the binding constant for Ca^{++} the same on both sides of the membrane, in spite of kinetic arguments to the contrary (Jencks, 1982). (The possible need to relinquish this constraint, at least for squid axon, is dis-

cussed later.) Similarly, for the sake of simplicity, we made the same constraint for the Na^+ binding constants, in spite of there being some experimental evidence to the contrary for isolated cardiac sarcolemmal vesicles (Philipson & Nishimoto, 1982). On the other hand, in the squid axon, Requena (1978) found that the half-affinity constant for extracellular Na^+ (41 mM) was similar to that for intracellular Na^+ (34 mM). The extracellular $[Ca^{++}]$ in the two cases was different, however, being 10 μM in the former and 10 mM for the latter.

We assumed that the process of ion-binding to the sites was diffusion limited and therefore set the association rate constant for Na^+ and Ca^{++} to the reasonably upper limit of 10^8 M^{-1} sec^{-1}. We also assumed that the Na^+-binding sites were independent, so that binding (association) of Na^+ to the enzyme with three empty sites was three times more probable (two times with one filled site) than with one empty site—similarly, but *vice versa*, for unbinding (dissociation). Given the fixed value for the association rate constant, the choice of dissociation rate constants for Ca^{++} and Na^+ was in effect determined by the binding constants for these ions. As will be shown (*see* Results) these were determined mainly by the experimentally observed values for the $K_{0.5}$ for Ca_i^{++}-activated and Na_o^+-activated Ca^{++} efflux, respectively.

Rate Constants for the Translocational Steps

Having chosen a symmetrical enzyme with regard to ion-binding affinities, at least as a starting point, we extended this concept (again on the grounds of simplicity) to the two remaining steps in the reaction schemes by requiring the equilibrium constants (neglecting the influence of voltage) for the two translocation steps be equal which, given the other constraints, required that they both equal unity. In other words, the forward and reverse rate constants for both translocational steps were made identical and were set equal to $10^5 \cdot sec^{-1}$, a value that was considered to be a reasonable upper limit (Tanford, *personal communication*).

Voltage Dependence

Given a stoichiometry of 3 Na^+ : 1 Ca^{++}, the exchange process must be electrogenic and therefore a function of transmembrane potential such that at equilibrium the exchange satisfy the thermodynamic requirement:

$$\frac{[Ca^{++}]_o \cdot [Na^+]_i^3}{[Ca^{++}]_i \cdot [Na^+]_o^3} = \exp(-FV/RT) \quad (1)$$

where V is the potential of the inside with respect to that of the outside. That is to say, one or more steps in the reaction sequence must be a function of membrane potential. As in the case of the electrogenic Na^+,K^+ transport mechanism (Chapman et al., 1983), it seemed reasonable to assign such voltage-dependence to one (or both) of the two translocational steps. Three versions of the simultaneous scheme were therefore studied, one with voltage dependence assigned to the ion-bound form of the enzyme (Step 11 in Fig. 1), one with it assigned to the unfilled form (Step 22 in Fig. 1) and one with it assigned to both forms, these three schemes being given the names, SIMV11, SIMV22, and SIMV1122, respectively. Similarly, in the consecutive mechanism of Fig. 2, the voltage dependence was either assigned to the Ca^{++}-filled step (Step 2 of Fig. 2) or to the Na^+-filled (Step 7 of Fig. 2) or to both, these three forms being given the names SEQV2, SEQV7 and SEQV27, respectively. For reasons previously discussed (Chapman et al., 1983), in each case the voltage dependence was distributed evenly over the forward and reverse rate constant of the step, multiplying the forward and dividing the reverse rate constant by $\exp(-FV/2RT)$, respectively, or by $\exp(-FV/4RT)$ when both translocational steps were made voltage dependent.[2]

Materials and Methods

Reaction Rate Laws

Simultaneous Mechanism

The following mass action rate laws were used for each of the 22 possible reaction steps involving the 16 enzyme intermediates as shown schematically in Fig. 1:

$$rf_1 = 3k_{on}[Na^+]_o[E] \quad (2)$$
$$rb_1 = (k_{on}/Na_B^{Na})[Na \cdot E] \quad (3)$$
$$rf_2 = 2k_{on}[Na^+]_o[Na \cdot E] \quad (4)$$
$$rb_2 = 2(k_{on}/Na_B^{Na})[Na_2 \cdot E] \quad (5)$$
$$rf_3 = k_{on}[Na^+]_o[Na_2 \cdot E] \quad (6)$$
$$rb_3 = 3(k_{on}/Na_B^{Na})[Na_3 \cdot E] \quad (7)$$
$$rf_4 = 3k_{on}[Na^+]_o[Ca \cdot E] \quad (8)$$
$$rb_4 = (k_{on}/Na_B^{Na})[Na \cdot Ca \cdot E] \quad (9)$$
$$rf_5 = 2k_{on}[Na^+]_o[Na \cdot Ca \cdot E] \quad (10)$$
$$rb_5 = 2(k_{on}/Na_B^{Na})[Na_2 \cdot Ca \cdot E] \quad (11)$$
$$rf_6 = k_{on}[Na^+]_o[Na_2 \cdot Ca \cdot E] \quad (12)$$

[2] For the definition of forward and reverse rates see the rate equations for the mechanisms of Figs. 1 & 2 listed in Materials and Methods.

$$rb_6 = 3(k_{on}/Na_B^{Na})[Na_3 \cdot Ca \cdot E] \quad (13)$$
$$rf_7 = k_{on}[Ca^{++}]_i[E] \quad (14)$$
$$rb_7 = (k_{on}/K_B^{Ca})[Ca \cdot E] \quad (15)$$
$$rf_8 = k_{on}[Ca^{++}]_i[Na \cdot E] \quad (16)$$
$$rb_8 = (k_{on}/K_B^{Ca})[Na \cdot Ca \cdot E] \quad (17)$$
$$rf_9 = k_{on}[Ca^{++}]_i[Na_2 \cdot E] \quad (18)$$
$$rb_9 = (k_{on}/K_B^{Ca})[Na_2 \cdot Ca \cdot E] \quad (19)$$
$$rf_{10} = k_{on}[Ca^{++}]_i[Na_3 \cdot E] \quad (20)$$
$$rb_{10} = (k_{on}/K_B^{Ca})[Na_3 \cdot Ca \cdot E] \quad (21)$$
$$rf_{11} = kf_1[Na_3 \cdot Ca \cdot E] \quad (22)$$
$$rb_{11} = kb_1[Na_3 \cdot Ca \cdot E'] \quad (23)$$
$$rb_{12} = k_{on}[Ca^{++}]_o[Na_3 \cdot E'] \quad (24)$$
$$rf_{12} = (k_{on}/K_B^{Ca})[Na_3 \cdot Ca \cdot E'] \quad (25)$$
$$rb_{13} = k_{on}[Ca^{++}]_o[Na_2 \cdot E'] \quad (26)$$
$$rf_{13} = (k_{on}/K_B^{Ca})[Na_2 \cdot Ca \cdot E'] \quad (27)$$
$$rb_{14} = k_{on}[Ca^{++}]_o[Na \cdot E'] \quad (28)$$
$$rf_{14} = (k_{on}/K_B^{Ca})[Na \cdot Ca \cdot E'] \quad (29)$$
$$rb_{15} = k_{on}[Ca^{++}]_o[E'] \quad (30)$$
$$rf_{15} = (k_{on}/K_B^{Ca})[Ca \cdot E'] \quad (31)$$
$$rb_{16} = k_{on}[Na^+]_i[Na_2 \cdot Ca \cdot E'] \quad (32)$$
$$rf_{16} = 3(k_{on}/Na_B^{Na})[Na_3 \cdot Ca \cdot E'] \quad (33)$$
$$rb_{17} = 2k_{on}[Na^+]_i[Na \cdot Ca \cdot E'] \quad (34)$$
$$rf_{17} = 2(k_{on}/Na_B^{Na})[Na_2 \cdot Ca \cdot E'] \quad (35)$$
$$rb_{18} = 3k_{on}[Na^+]_i[Ca \cdot E'] \quad (36)$$
$$rf_{18} = (k_{on}/Na_B^{Na})[Na \cdot Ca \cdot E'] \quad (37)$$
$$rb_{19} = k_{on}[Na^+]_i[Na_2 \cdot E'] \quad (38)$$
$$rf_{19} = 3(k_{on}/Na_B^{Na})[Na_3 \cdot E'] \quad (39)$$
$$rb_{20} = 2k_{on}[Na^+]_i[Na \cdot E'] \quad (40)$$
$$rf_{20} = 2(k_{on}/Na_B^{Na})[Na_2 \cdot E'] \quad (41)$$
$$rb_{21} = 3k_{on}[Na^+]_i[E'] \quad (42)$$
$$rf_{21} = (k_{on}/Na_B^{Na})[Na \cdot E'] \quad (43)$$
$$rf_{22} = kf_2[E'] \quad (44)$$
$$rb_{22} = kb_2[E] \quad (45)$$

where rf_i, rb_i are the forward and reverse rates of the ith step. k_{on} is the ion association rate (on rate) constant, Na_B^{Na} and Ca_B^{Ca} are the Na^+ and Ca^{++} binding constants, respectively; kf_1, kf_2 and kb_1, kb_2 are the forward and reverse rate constants for the two translocational steps, respectively. Voltage dependence was ascribed to step 11 or step 22 by multiplying and dividing, respectively, the forward and reverse rate constants for either step by $\exp(-FV/2RT)$, or in the case of assigning voltage dependence to both steps, by $\exp(-FV/4RT)$.

Consecutive Mechanism

The following mass action rate laws were used for each of the ten reaction steps involving the ten intermediates shown in Fig. 2:

$$rf_1 = k_{on}[Ca^{++}]_i[E] \quad (46)$$
$$rb_1 = (k_{on}/K_B^{Ca})[Ca \cdot E] \quad (47)$$
$$rf_2 = kf_1[Ca \cdot E] \quad (48)$$
$$rb_2 = kb_1[Ca \cdot E'] \quad (49)$$
$$rf_3 = (k_{on}/K_B^{Ca})[Ca \cdot E'] \quad (50)$$
$$rb_3 = k_{on}[Ca^{++}]_o[E'] \quad (51)$$
$$rf_4 = 3k_{on}[Na^+]_o[E'] \quad (52)$$
$$rb_4 = (k_{on}/K_B^{Na})[Na \cdot E'] \quad (53)$$
$$rf_5 = 2k_{on}[Na^+]_o[Na \cdot E'] \quad (54)$$
$$rb_5 = 2(k_{on}/K_B^{Na})[Na_2 \cdot E'] \quad (55)$$
$$rf_6 = k_{on}[Na^+]_o[Na_2 \cdot E'] \quad (56)$$
$$rb_6 = 3(k_{on}/K_B^{Na})[Na_3 \cdot E'] \quad (57)$$
$$rf_7 = kf_2[Na_3 \cdot E'] \quad (58)$$
$$rb_7 = kb_2[Na_3 \cdot E] \quad (59)$$
$$rf_8 = 3(k_{on}/K_B^{Na})[Na_3 \cdot E] \quad (60)$$
$$rb_8 = k_{on}[Na^+]_i[Na_2 \cdot E] \quad (61)$$
$$rf_9 = 2(k_{on}/K_B^{Na})[Na_2 \cdot E] \quad (62)$$
$$rb_9 = 2k_{on}[Na^+]_i[Na \cdot E] \quad (63)$$
$$rf_{10} = (k_{on}/K_B^{Na})[Na \cdot E] \quad (64)$$
$$rb_{10} = k_{on}[Na^+]_i[E] \quad (65)$$

where k_{on}, K_B^{Ca}, K_B^{Na}, kf_1, kf_2, kb_1 and kb_2 have the same meaning as for the simultaneous mechanism described above. Voltage dependence was ascribed to step 2 or step 7 by multiplying and dividing, respectively, the forward and reverse rare constants for either step by $\exp(-FV/2RT)$, or in the case of assigning voltage dependence to both steps, by $\exp(-FV/4RT)$.

Computational Methods

The dimensions of the rate coefficients listed in the Table are those appropriate to yield rate of reaction in mol · cm^{-2} · sec^{-1}. Steady-state solutions for the concentrations of the intermediates were obtained by Gaussian elimination and used to solve for the unidirectional rates of each of the reaction steps. The model equations were programmed in C (Kernighan & Ritchie, 1978) and compiled and linked to a general purpose simulation software package SCoP (Holt & Kootsey, 1984) using the Optimizing C86 compiler (Computer Innovations, Inc., Tinton Falls, N.J.) and IBM PC-DOS linker running on an IBM PC-XT (IBM, Boca Raton, Florida) equipped with an Intel 8087 floating point hardware chip.[3]

As a safety check on the computations a 0.01% tolerance was placed on the required agreement between the following pairs of quantities:

1. The sum of the computed enzyme intermediates and the set parameter for total enzyme per unit area of membrane;

2. The net steady-state rate of reaction calculated as the difference between the overall unidirectional forward and reverse rates (calculated as described below) and the net steady-

[3] The complete software package (SIMV11 together with SCoP) is available to the interested reader by writing to Dr. J. Mailen Kootsey, National Biomedical Simulation Resource, Duke University Medical Center, P.O. Box 3709, Durham, N.C. 27710, USA.

state rate calculated as the difference between the unidirectional forward and reverse rates of reaction step 11 or 22 of Fig. 1.

Calculation of Unidirectional Reaction Rates

The overall unidirectional forward and reverse rates of a multistep reaction are functions of the unidirectional forward and reverse rates of the elementary steps comprising the reaction, which for the random ion-binding mechanism of Fig. 1 are especially complex. The unidirectional Ca^{++} fluxes were calculated by reducing the multiple branching pathways for unidirectional Ca^{++} exchange to a single equivalent reaction step by the application of the following rule (E.A. Johnson, *to be published*). The equivalent single unidirectional forward rate Rf over any two successive elementary reaction steps, with unidirectional forward and reverse rates rf_1, rf_2, rb_1 and rb_2, respectively, is given by:

$$Rf = rf_1 \frac{rf_2}{rf_2 + rb_1} \tag{66}$$

and similarly, the equivalent single unidirectional backward rate Rb is given by the product of rb_1 and rb_2 divided by the same denominator. It can be seen that a series of reaction steps 1, 2, 3, 4, e.g., can be reduced to an overall single equivalent step by first reducing steps 1 and 2 to a single equivalent step using the above rule. One then reduces that step and the next elementary step (step 3) to another equivalent single step by using the rule again, and so on. Branches are dealt with by first reducing the limbs of each branch to equivalent single steps up to the branch point, at which stage the two equivalent unidirectional forward and reverse rates, respectively, are simply summed, the above procedure being repeated with the following elementary step if the reaction sequence continues beyond the branch point.

Results and Discussion

As pointed out above, the mechanisms of Na^+–Ca^{++} exchange that we chose to study are of the minimum degree of complexity and hence undoubtedly simpler than the actual mechanism. Consequently, it should not be surprising to find that the mechanisms fail to account for all experimental results. Furthermore, many of the experimental preparations in which Na^+–Ca^{++} exchange has been studied have at least one other Ca^{++} transporting mechanism (as well as other exchange mechanisms), a Ca^{++}-ATPase, driven by the free energy available from the splitting of ATP, which may in part be responsible for some of the behavior ostensibly attributed to Na^+–Ca^{++} exchange. As a consequence our emphasis here will be more on the ability, rather than the inability, of a particular mechanism to account for experimental data. In addition we have not attempted to explore to any significant degree what modifications might be required of any mechanism to extend the range of data that it might fit. Indeed, before addressing such an issue one would need a more quantitative estimate of a given mechanism's ability or inability to fit a certain set of data than that provided by a trial and error sampling of the large number of possible sets of parameter values that are possible, even for the minimum mechanisms studied here. That is to say we would need to make a more systematic search of the parameter space for each mechanism, a process best performed by computer and a more appropriate subject for a separate investigation.

Table

Parameter	Value	Units
Total [enzyme]	2×10^{-14}	mols · cm^{-2}
K_{on}	10^8	$M^{-1} \cdot sec^{-1}$
K_B^{Ca}	10^6	M^{-1}
K_B^{Na}	12	M^{-1}
kf_1	10^5	sec^{-1}
kb_1	10^5	sec^{-1}
kf_2	10^5	sec^{-1}
kb_2	10^5	sec^{-1}

Given these considerations, we have focused our attention on the behavior of one of the three simultaneous mechanisms that we have studied, namely, SIMV11, i.e., the mechanism with voltage-dependence solely on the step involving the translocation of the ion-filled form of the enzyme (step [11] in Fig. 1). Much of the experimental data fitted by this mechanism may have been equally well-fitted (perhaps better) by the other simultaneous schemes (SIMV22 and SIMV1122, i.e., voltage dependence on the unfilled translocational form, or on both translocational forms of the enzyme). We found the fit of SIMV11 to the experimental data sufficiently satisfactory at the present level of investigation to preclude the necessity of a comparative exploration of the behavior of the various simultaneous mechanisms described here. The consecutive schemes (SEQV2, SEQV7 and SEQV27, i.e., mechanisms with voltage-dependence on the Ca^{++}-filled, Na^+-filled, or both translocational forms of the enzyme, respectively) were not studied in any detail other than to illustrate specific points of possible fundamental difference between them and the simultaneous schemes that are the focus of the present paper. Again, in this regard, we stress that these differences are merely ones that we discovered in our exploration of the general behavior of the mechanisms and are not the result of a systematic comparative study.

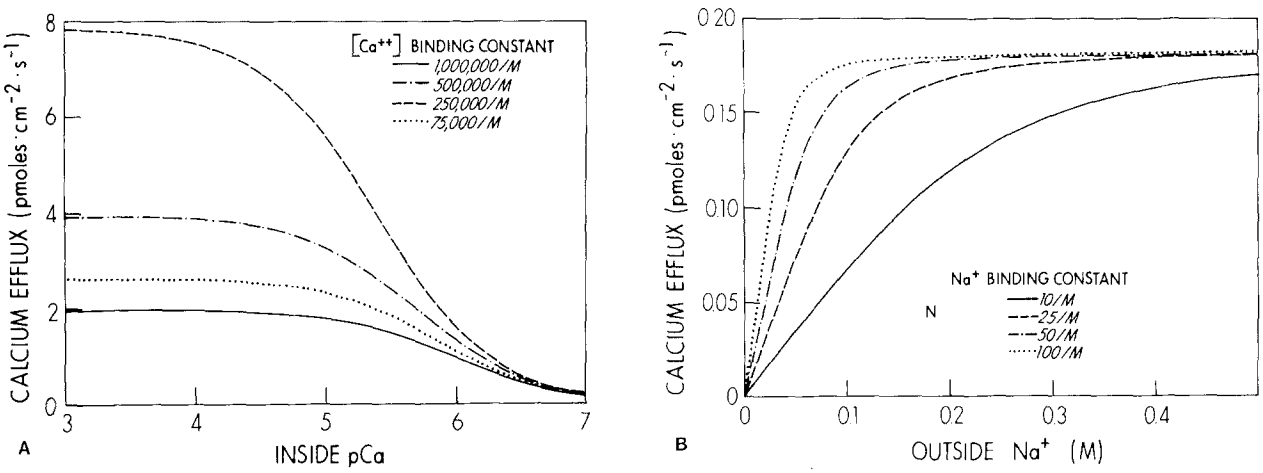

Fig. 3. Effect of changing (*A*) K_B^{Ca} (values listed in the figure) on the activation of Ca^{++} efflux by Ca_i^{++} and (*B*) changing K_B^{Na} (values listed in the figure) on the activation of Ca^{++} efflux by Na_o^+. Boundary conditions appropriate for the dialyzed squid axon preparation of Blaustein (1977): $[Ca^{++}]_o$ = 12 μM, $[Na^+]_i$ = 5 mM, transmembrane potential = −60 mV, T = 15°C. $[Na^+]_o$ in (*A*) = 425 mM, $[Ca^{++}]_i$ in (*B*) = 0.1 μM. All other constants and parameters as in the Table

Establishing a Set of Rate Constants and Enzyme Density

Given the assumptions and constraints discussed in the Mechanism section above, only two (out of the possible total of 19) arbitrarily adjustable rate constants remained to be chosen. These were the binding constants for Ca^{++} (K_B^{Ca}) and Na^+ (K_B^{Na}), each of which was assumed to have the same value on each side of the membrane. In spite of these severe constraints it was found that a great deal of the experimental data in the literature could be reproduced using a small range of values for these two binding constants, without any need to modify or relax these constraints. As a prelude to illustrating the general features of the behavior of SIMV11 in the following section, Fig. 3 shows the effects of varying the two ion-binding constants over an approximately ± threefold range on the activation of Ca^{++} efflux by intracellular Ca^{++} and extracellular Na^{++}, respectively, for boundary conditions appropriate for the dialyzed squid axon preparation (e.g. the experiments of Blaustein, 1977). The only remaining adjustable parameter, the density of enzyme in the membrane, merely scales the magnitude of the activity of the exchanger; it does not in any way affect the form of the dependence of the activity on any of the other parameters. In Fig. 3 (and in all of the remaining figures) the density was set at 20 fmol/cm^2, which corresponds to approximately 120 exchanger molecules per square micron, a density about one order of magnitude less than that of the sarcolemmal Na,K-ATPase of cardiac muscle (Michael et al., 1979; Daut & Rudel, 1981) and skeletal muscle (Venosa & Horowicz, 1981).

Examples of the General Behavior of the Enzyme

Ca^{++} Efflux: Ionic and Voltage Dependences

Activation by Intracellular Ca^{++}. Figure 4*A* shows activation of unidirectional Ca^{++} efflux by $[Ca^{++}]_i$ under ionic conditions corresponding to those employed by Blaustein (1977) for the dialyzed squid giant axon. A K_B^{Ca} of 10^6 M^{-1} was chosen to give a $K_{0.5}$ for $[Ca^{++}]_i$ of around 1 μM, in keeping with the value obtained experimentally (the value of K_B^{Na} was the same as that used in Fig. 5*A*, *see below*).

Using the same values of K_B^{Ca} and of K_B^{Na} that were used in Fig. 4*A*, but matching the ionic conditions commonly used to study Ca^{++} uptake into Na^+-loaded cardiac sarcolemmal vesicles, Fig. 4*B* shows Ca^{++} uptake as a function of extravesicular $[Ca^{++}]$. Although the extravesicular ion composition is relatively well controlled in such experiments, the intravesicular composition is not, especially the intravesicular $[Ca^{++}]$ which changes rapidly during the course of Ca^{++} uptake. For example, taking an intravesicular volume of 20 μl/mg of vesicular protein (Bers et al., 1980) and a modest uptake rate of 2 nmol Ca^{++}/mg protein/sec, the rate of change of intravesicular $[Ca^{++}]$ would be 0.1 mM/sec, and corresponding greater for the higher up-

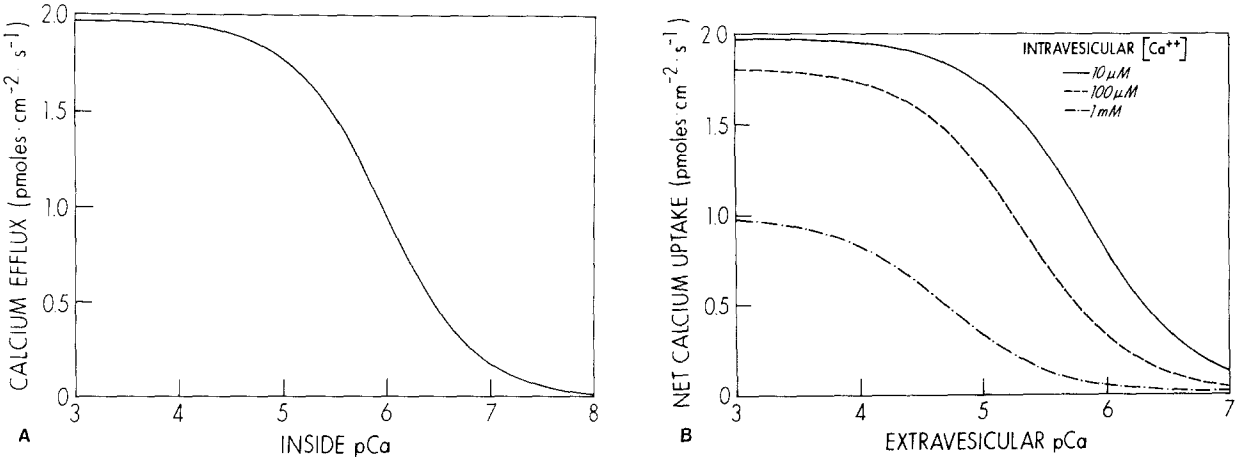

Fig. 4. (*A*) Unidirectional Ca^{++} efflux as a function of inside $[Ca^{++}]$. The ionic parameters were chosen to match the experimental conditions of Blaustein (1977; *cf.* his Fig. 8) with the squid giant axon. $[Na^+]_o$ = 425 mM, $[Na^+]_i$ = 5 mM, $[Ca^{++}]_o$ = 12 μM (nominally zero) and a transmembrane potential of −65 mV was assumed. T = 15°C. For these experimental conditions, since there is negligible unidirectional Ca^{++} influx, the unidirectional efflux is equivalent to net flux. All rate constants and other parameters as in the Table. (*B*) Unidirectional Ca^{++} uptake into Na^+-loaded cardiac sarcolemmal vesicles as a function of extravesicular $[Ca^{++}]$, for the 3 values of intravesicular $[Ca^{++}]$ listed in the figure. Intravesicular $[Na^+]$ = 160 mM, extravesicular $[Na^+]$ = 0.1 mM (nominally zero), extravesicular $[Ca^{++}]$ = 15 μM, transmembrane potential = 0 mV and T = 37°C. All rate constants and other parameters as in the Table

take rates of 15 to 20 nmol/mg/sec reported by Caroni et al. (1980) and Caroni and Carafoli (1983) for fully activated (phosphorylated) vesicles (*cf.* their Fig. 3). As can be seen from Fig. 4*B*, the form and magnitude of the Ca^{++} uptake depends markedly on the intravesicular $[Ca^{++}]$, the $K_{0.5}$ increasing with increasing intravesicular $[Ca^{++}]$. This effect of varying intravesicular $[Ca^{++}]$ could explain the extraordinarily wide range of $K_{0.5}$ values reported in the literature for activation of Ca^{++} uptake by extravesicular Ca^{++} [*cf.* Reeves and Sutko (1983), who cite 1.5 to 140 μM as the range they found in previously published studies].

The behavior shown in Fig. 4*B* also illustrates the marked difference in the behavior of the mechanism of Fig. 1 (SIMV11) and its simplified variant (SIMV5), referred to in footnote [1]. The form and magnitude of Ca^{++} uptake with SIMV5, under exactly the same boundary conditions, and using the same binding and translocational rate constants as with SIMV11 in Fig. 4*B*, is virtually unaffected (<1% variation in V_{max} and $K_{0.5}$) by changes in intravesicular $[Ca^{++}]$ over the same range of 10^{-5} to 10^{-3} M. A similar discrepancy in behavior between these two mechanisms will be described in the following section.

Activation by Extracellular Na^+. Figure 5*A* shows the dependence of unidirectional Ca^{++} efflux on extracellular $[Na^+]$ at three values of intracellular $[Ca^{++}]$ for conditions matching the experiments of Blaustein (1977) (*cf.* his Fig. 10*A*) with the dialyzed squid axon preparation. A K_B^{Na} of 12 M^{-1} was chosen to give a $K_{0.5}$ for Na_o^+ of ≈ 50 mM for the efflux curve at an intracellular $[Ca^{++}]$ of 2.5 μM, in accordance with the value obtained experimentally by Blaustein (1977). This value for the $K_{0.5}$ for Na_o^+ is considerably lower than that found by others, e.g., DiPolo and Beauge (1981; *cf.* their Fig. 10). As will be shown later this variation in $K_{0.5}$ for Na_o^+ can be accounted for by the different intracellular $[Na^+]$ used by these and other workers and is entirely consistent with the value of 12 M^{-1} for K_B^{Na} used in Fig. 5*A*.

Figure 5*B* shows net Ca^{++} uptake as a function of intravesicular $[Na^+]$ for ionic conditions matching those of experiments with isolated cardiac sarcolemmal vesicles (Reeves & Sutko, 1983). As mentioned above in the previous section, the intravesicular $[Ca^{++}]$ would be expected to increase rapidly as Ca^{++} uptake proceeded. As shown in the figure, the Ca^{++} uptake curve with changing intravesicular $[Na^{++}]$ is markedly influenced by the intravesicular $[Ca^{++}]$, the $K_{0.5}$ for uptake increasing as intravesicular $[Ca^{++}]$ increases. These findings are in striking agreement with those of Reeves and Sutko (1983) who observed that when the rate of $[Ca^{++}]$ uptake was measured over an initial 1-sec interval, the uptake rate increased rapidly with increasing intravesicular $[Na^+]$ ($K_{0.5}$ = 26 mM). On the other hand, when the measurement interval was increased to 10 sec (when the intravesicular

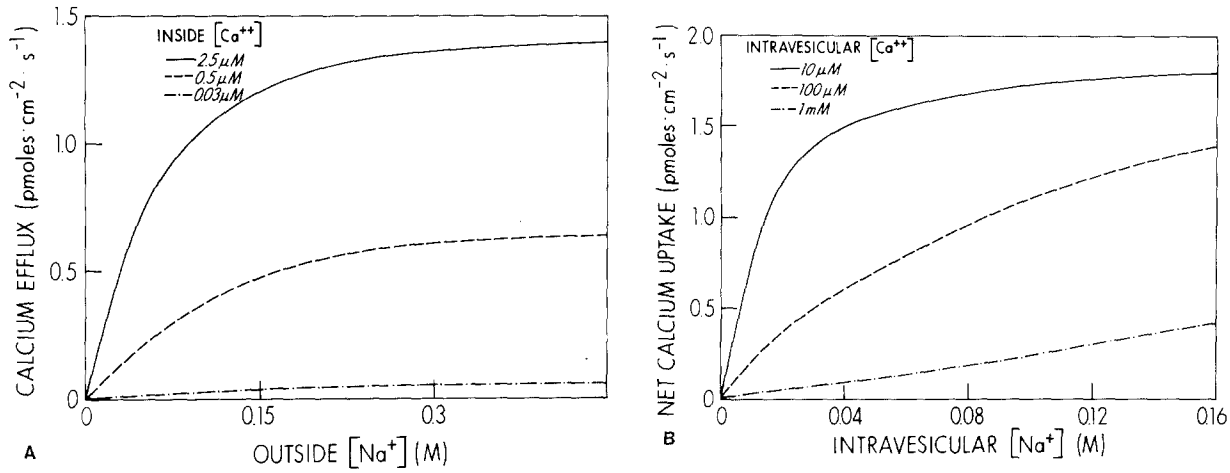

Fig. 5. (*A*) Unidirectional Ca^{++} efflux as a function of extracellular $[Na^+]$, for the 3 values of $[Ca^{++}]_i$ listed in the figure. The ionic parameters were chosen to match the experimental conditions of Blaustein (1977; *cf.* his Fig. 10*A*) with the squid giant axon. $[Na^+]_i = 5$ mM, $[Ca^{++}]_o = 10$ μM (nominally zero). A transmembrane potential of −65 mV was assumed. $T = 15$°C. $K_{0.5} \approx 50$ mM for the uppermost curve. All rate constants and other parameters as in the Table. (*B*) Net Ca^{++} uptake into cardiac sarcolemmal vesicles as a function of intravesicular $[Na^+]$, for the 3 values of intravesicular $[Ca^{++}]$ listed in the figure. Extravesicular $[Ca^{++}]$ and $[Na^+]$ were 15 μM and 0.1 mM (nominally zero), respectively. Membrane potential = 0 mV. $T = 37$°C. All rate constants and other parameters as in the Table

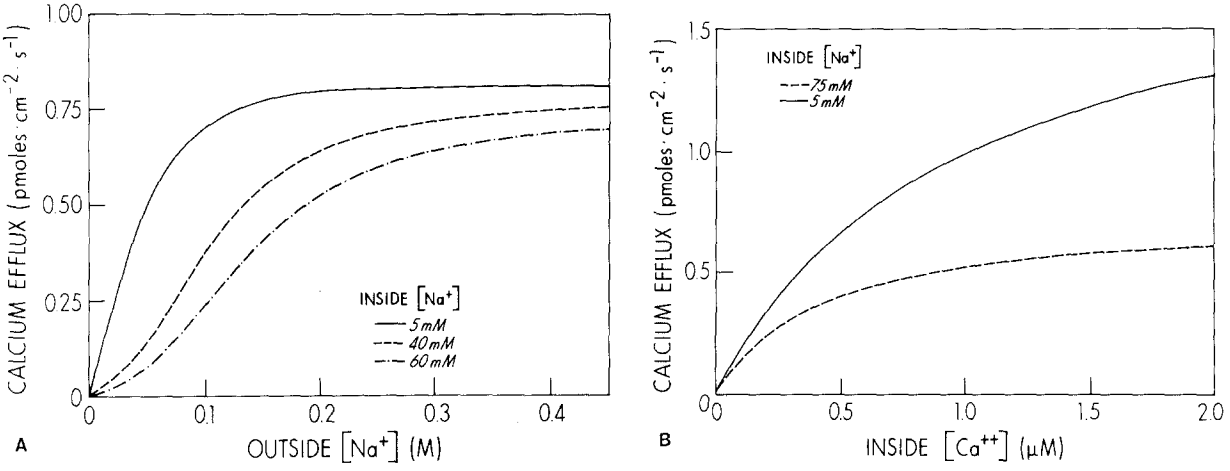

Fig. 6. (*A*) Influence of intracellular $[Na^+]$ on unidirectional Ca^{++} efflux as a function of extracellular $[Na^+]$. The ionic parameters were chosen to match those of squid axon experiments. $[Ca^{++}]_o = 10$ μM (nominally zero), $[Ca^{++}]_i = 0.7$ μM, and a transmembrane potential of −60 mV was assumed. $T = 15$°C. $K_B^{Na} = 30$ M^{-1}; all other rate constants and parameters as in the Table. (*B*) Ca^{++} efflux as a function of $[Ca^{++}]_i$ for the 2 values of $[Na^+]_i$ listed in the figure. $[Na^+]_o = 440$ mM, $[Ca^{++}]_o = 10$ μM (nominally zero). A transmembrane potential of −60 mV was assumed. $T = 15$°C. $K_B^{Na} = 60$ M^{-1}. All other rate constants and parameters as in the Table

$[Ca^{++}]$ must have risen to higher levels), the rate of Ca^{++} uptake became almost a linear function of intravesicular $[Na^+]$.

As illustrated in the previous section (Activation by Intracellular Ca^{++}), a simplified variant (SIMV5) of the mechanism of Fig. 1 (SIMV11) showed quite different behavior: Ca^{++} uptake as a function of intravesicular $[Na^+]$ was virtually independent of the intravesicular $[Ca^{++}]$ (10^{-5} to 10^{-3} M).

Effect of Intracellular $[Na^+]$. In the squid axon, increasing intracellular $[Na^+]$ markedly inhibits Ca^{++} efflux. This property is also shared by SIMV11, as is shown in Fig. 6*A* where unidirectional Ca^{++} efflux is plotted as a function of extracellular $[Na^+]$ for various values of intracellular $[Na^+]$, including the value of 5 mM used by Blaustein (1977). The marked shift to the right along the abscissa for higher values of $[Na^+]_i$ is fully in accord with experimental findings, e.g. those of

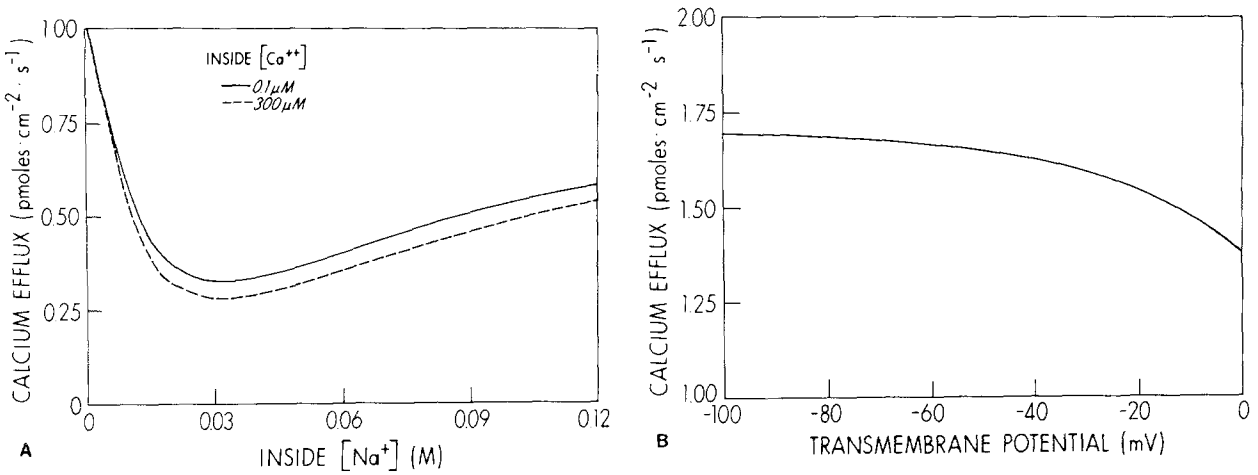

Fig. 7. (*A*) Dependence of unidirectional Ca^{++} efflux on $[Na^+]_i$ for the 2 values of $[Ca^{++}]_i$ listed in the figure. Ca^{++} efflux was normalized to the maximum flux obtained at nominally zero $[Na^+]_i$. Ionic parameters chosen to match squid axon experiments: $[Na^+]_o$ = 440 mM, $[Ca^{++}]_o$ = 10 mM, membrane potential = −60 mV, T = 15°C. K_B^{Na} = 30 M^{-1}; all other rate constants and parameters as in the Table. (*B*) Effect of transmembrane potential on unidirectional Ca^{++} efflux. Ionic parameters chosen to match squid axon experiments of Blaustein et al. (1974): $[Na^+]_o$ = 425 mM, $[Na^+]_i$ = 50 mM, $[Ca^{++}]_o$ = 10 μM (nominally zero), $[Ca^{++}]_i$ = 250 μM, T = 15°C K_B^{Na} = 30 M^{-1}; all other rate constants and parameters as in the Table

Blaustein et al. (1974) and of DiPolo and Beauge (1981) who found a $K_{0.5}$ for Na_o^+ of 125 mM at an intracellular $[Na^+]$ of 50 and 60 mM, respectively.

Figure 6*B* shows the effect of a change in intracellular $[Na^+]$ on unidirectional Ca^{++} efflux as a function of intracellular $[Ca^{++}]$ for ionic conditions matching those yielding the data of Blaustein (1977; Fig. 11); the behavior of SIMV11 is quite similar to the experimental findings in the squid axon. Figure 7*A* shows the corresponding dependence of Ca^{++} efflux on $[Na^+]_i$ for various values of intracellular $[Ca^{++}]$, normalized to the maximum Ca^{++} efflux obtained at nominally zero $[Na^+]_i$ (1 mM). The results are in good agreement with the findings in squid (Brinley et al., 1975, Fig. 10; Requena, 1978). Whether the small rise in efflux at the higher values of $[Na^+]_i$ seen in Fig. 7 occurs experimentally cannot be determined because of the scatter in the published data.

Effect of Extracellular $[Ca^{++}]$. Although Ca_o^{++}-dependent Ca^{++} efflux has been found under certain experimental conditions in the squid giant axon, little (if any) occurs under normal conditions (DiPolo & Beauge, 1980). Indeed, it has been proposed that most of the apparent dependence on Ca_o^{++} of the rate of loss of $^{45}Ca^{++}$ from unpoisoned axons is not the manifestation of a membrane Ca^{++} transport mechanism but of the properties of a superficial layer of Ca^{++} binding sites sandwiched between the axolemma and an extracellular barrier such as the Schwann cells (Baker & McNaughton, 1978). Nonetheless, when such binding sites are removed, in axons poisoned with dinitrophenol considerable Ca^{++}–Ca^{++} exchange develops which is activated by monovalent cations (Baker & McNaughton, 1978). No Ca_o^{++}-dependent Ca^{++} efflux was observed with SIMV11, the only effect of Ca_o^{++} being inhibitory; increasing $[Ca^{++}]_o$ decreased the unidirectional Ca^{++} efflux so that maximum values were obtained at the nominally zero concentration of 10 μM usually employed by Blaustein (*cf.* Blaustein, 1977) rather than at the higher concentrations employed by, e.g., DiPolo (1973) and others.

Such evidence for Ca^{++}–Ca^{++} exchange, also activated by various metal ions, has been found in cardiac sarcolemmal vesicles (Philipson & Nishimoto, 1981; Slaughter et al., 1983). We made no attempt at this stage to account for exchange of this kind, for it cannot be accounted for by SIMV11 and its derivatives without introducing unwanted net dissipative fluxes of Na^+ and/or Ca^{++}. One way out of this difficulty, and at the same time retaining the relative simplicity of the present mechanisms, is to suppose that other forms of the exchanger can exist in which translocation of the empty (ion-free) form of the enzyme is highly *improbable*. In which case all kinds of exchange, without net transport, might be accounted for. We preferred to delay pursuit of this possibility for a future occasion.

Effect of Transmembrane Potential. The possibility that stimulation of Ca_o^{++}-Na_i^+ exchange by external K^+ is due to the change in membrane potential was discussed by Baker (1972). Indeed, depolarization has been found to decrease Ca^{++} ef-

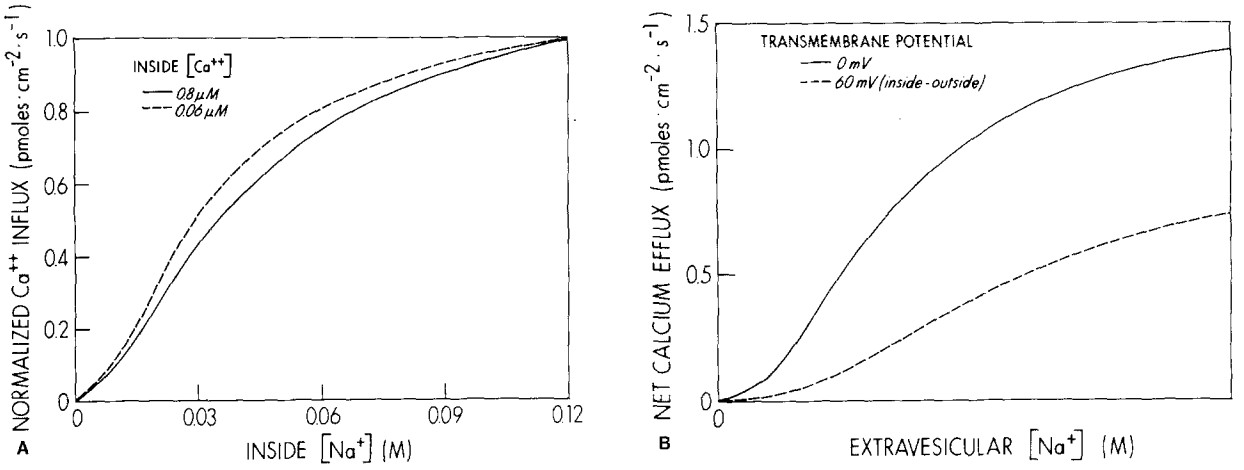

Fig. 8. (*A*) Dependence of normalized unidirectional Ca^{++} influx on $[Na^+]_i$ for the two values of $[Ca^{++}]_i$ listed in the figure. Ionic parameters chosen to match the experimental conditions of DiPolo (1979; *cf.* Fig. 4) with squid giant axon. $[Na^+]_o$ = 440 mM, $[Ca^{++}]_o$ = 10 mM, and a transmembrane potential of −60 mV was assumed. T = 15°C. The two curves have essentially the same $K_{0.5}$ of ≈60 mM, as found experimentally. K_B^{Na} = 60 M^{-1}, all other rate constants and parameters as in the Table. (*B*) Net Ca^{++} efflux from Na^+-loaded cardiac sarcolemmal vesicles as a function of extravesicular $[Na^+]$ with a transmembrane potential of either 0 or 50 mV (inside potential with respect to outside). Boundary conditions chosen to match those of Philipson and Nishimoto (1981). Extravesicular $[Ca^{++}]$ = 25 μM, intravesicular $[Na^+]$ = 140 mM, and the intravesicular $[Ca^{++}]$ was assumed to be nominally zero (10 μM). T = 37°C. K_B^{Na} = 30 M^{-1}; all other rate constants and parameters as listed in the Table

flux in squid axon (Blaustein et al., 1974; Mullins & Brinley, 1975; Baker & McNaughton, 1976*a*,*b*; Allen & Baker, 1983). Figure 7*B* shows the effect of membrane potential on SIMV11 for ionic conditions (*see* figure legend) corresponding to the experiments of Blaustein et al. (1974) and similar to those of Allen and Baker (1983) on squid axon. Essentially similar results were obtained with voltage-dependence on the empty (ion-free) form of the enzyme (SIMV22), except the dependency was more marked in the physiological range of potentials and in that regard could be said to be more in keeping with the experimental results. No attempt was made, however, to adjust model parameters such as the relative values of the rate constants of the translocational steps to explore whether one or other mechanism was to be preferred. As will be shown later, the effects of membrane potential on unidirectional ion fluxes can be either large or small, inhibitory or stimulatory, depending on the ionic boundary conditions.

Ca^{++} Influx: Ionic and Voltage Dependences

Effect of Intracellular $[Na^+]$. Whereas intracellular Na^+ inhibits Ca^{++} efflux it stimulates Ca^{++} influx dramatically, a characteristic of Na^+–Ca^{++} exchange that has been demonstrated in squid axon in many studies (Baker et al., 1969; DiPolo, 1979). Figure 8*A* shows this behavior in SIMV11, where the boundary conditions were set to match those of DiPolo (1979) with squid axon. The $K_{0.5}$ of 60 mM is close to that observed experimentally as is the effect of a change in intracellular $[Ca^{++}]$ which left the $K_{0.5}$ essentially unchanged. DiPolo (1979), however, found that the foot of the activation curve became more sigmoidal at lower internal $[Ca^{++}]$. This feature was not reproduced by SIMV11, although no attempt was made to explore whether a change in model parameters might have enabled it to do so. A particularly striking similarity in behavior of SIMV11 and squid axon is that the maximum Ca^{++} influx via Na^+–Ca^{++} exchange under conditions of high activating Na_i^+ and saturating Ca_o^{++} is about one-tenth that of Ca^{++} efflux, at high activating Ca_i^{++} and saturating Na_o^+. Requena and Mullins (1979) found this finding in squid axon puzzling.

Figure 8B shows the effect of extravesicular $[Na^+]$ on Ca^{++} efflux from cardiac vesicles. Note that the efflux rate is enhanced by a positive transmembrane potential, which would be developed during the time-course of the efflux. This might account for the sharp sigmoidicity of the corresponding experimental curve observed by Philipson and Nishimoto (1981).

Effect of Extracellular $[Ca^{++}]$. As can be seen from Fig. 9*A*, the $K_{0.5}$ for activation of unidirectional Ca^{++} influx by Ca_o^{++} with SIMV11 (boundary conditions for squid axon) is higher (≈50 μM) than the $K_{0.5}$ for activation of Ca^{++} efflux by $[Ca^{++}]_i$ (≈1

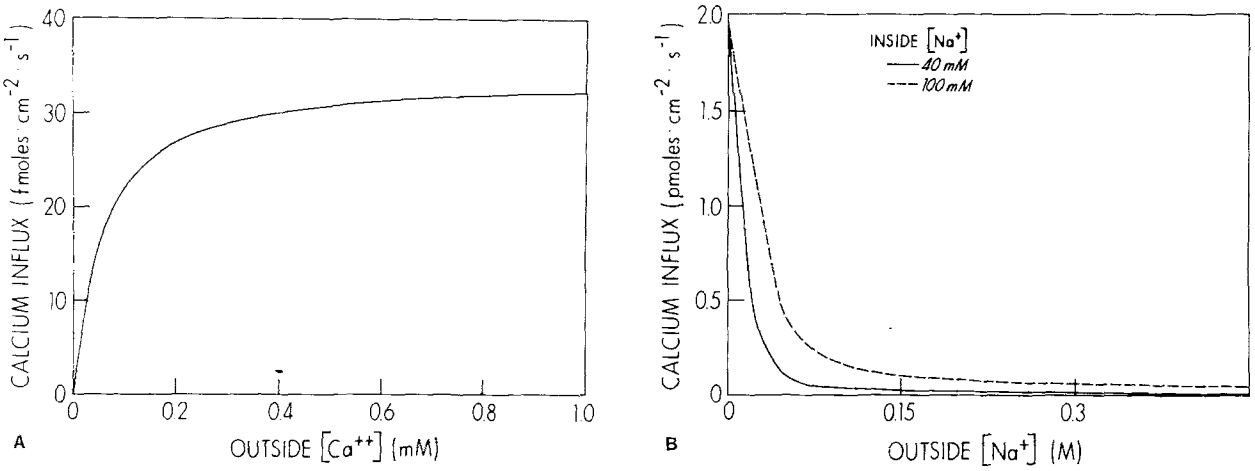

Fig. 9. (*A*) Dependence of unidirectional Ca^{++} influx on outside $[Ca^{++}]$. Ionic parameters chosen to match squid axon experiments of Baker et al. (1969): $[Na^+]_o$ = 442 mM, $[Na^+]_i$ = 80 mM, $[Ca^{++}]_i$ = 1 μM, T = 15°C. A membrane potential of −60 mV was assumed. All rate constants and other parameters as in the Table. (*B*) Dependence of unidirectional Ca^{++} influx on $[Na^+]_o$, for the two values of $[Na^+]_i$ listed in the figure. Ionic parameters chosen to match squid axon experiments of Baker et al. (1969): $[Ca^{++}]_o$ = 11 mM, $[Ca^{++}]_i$ = 1 μM, T = 15°C, membrane potential = −60 mV. All rate constants and other parameters as in the Table

μM) (*compare* Fig. 9*A* with Fig. 4*A*), although the $K_{0.5}$ is not as high as that observed experimentally for the corresponding dependence of Na^+ efflux (Baker et al., 1969). This finding may require one to relinquish, at least for the squid axon, the constraint that the Ca^{++} binding constant on the two sides of the membrane be the same. However, we did not pursue this, or other possibilities, at this stage.

Effect of Extracellular $[Na^+]$. As was shown by Baker et al. (1969) in squid axon, Ca^{++} influx is markedly inhibited by extracellular Na^+. Such behavior is also shown by SIMV11 as illustrated in Fig. 9*B*, where unidirectional Ca^{++} influx is shown as a function of extracellular $[Na^+]$ for two values of $[Na^+]_i$ and for ionic conditions appropriate for their experiments.

Effect of Transmembrane Potential. Figure 10 shows net Ca^{++} flux exhibited by SIMV11 as a function of membrane potential for two different values of intracellular $[Na^+]$, corresponding to those used by Mullins et al. (1983) in experiments with squid axon. The resemblance of the voltage-dependence of net Ca^{++} flux shown in the figure to that observed by these authors is quite striking. Ca^{++} influx is noticeable in Fig. 10 at potentials somewhat more negative than those at which influx was measured experimentally. This could perhaps be accounted for if the plasmalemmal Ca-ATPase in squid was effective in extruding the relatively small influx of Ca^{++} via Na^+–Ca^{++} exchange at these negative potentials, so that a net influx was not detectable until

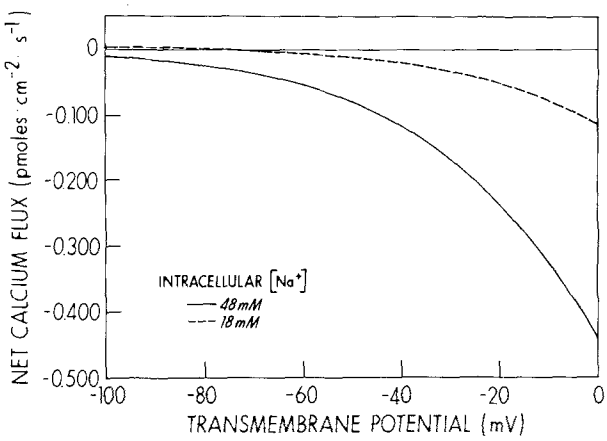

Fig. 10. Dependence of net Ca^{++} flux on transmembrane potential for the two values of $[Na^+]_i$ listed in the figure. Ionic parameters chosen to match squid axon experiments of Mullins et al. (1983): $[Ca^{++}]_o$ = 3 mM, $[Ca^{++}]_i$ = 0.1 μM, $[Na^+]_o$ = 200 mM. T = 20°C. K_B^{Na} = 30 M^{-1}; all other constants and parameters as in the Table

the Ca-ATPase became saturated by the greater influx through the exchanger at more depolarized potentials. That is to say, the net Ca^{++} uptake recorded by Mullins et al. (1983) was the difference between an influx via Na^+–Ca^{++} exchange and an efflux via the plasmalemmal Ca^{++} pump. Allen and Baker (1983) observed a similar stimulation of unidirectional Ca^{++} influx with membrane depolarization (*see* General Considerations: Net and Unidirectional Fluxes: Effect of Transmembrane Potential).

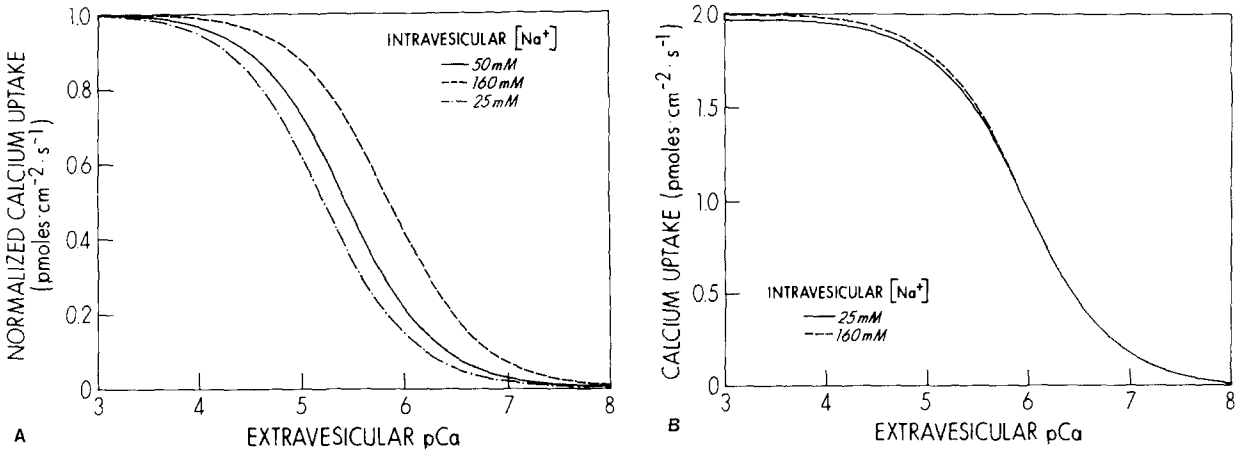

Fig. 11. (*A*) Activation of Ca^{++} uptake by extravesicular Ca^{++} for the 3 values of intravesicular $[Na^+]$ listed in the figure. Conditions made to resemble those of Ledvora and Hegyvary (1983) for cardiac sarcolemma vesicles. Extravesicular $[Na^+]$ = 1 mM (nominally zero), intravesicular $[Ca^{++}]$ = 10 μM (nominally zero), extravesicular $[Ca^{++}]$ = 17 μM, membrane potential assumed = 0 mV, T = 15°C. All rate constants and other parameters as in the Table. (*B*) Consecutive mechanism: Activation of Ca^{++} uptake by extravesicular Ca^{++} for the two extreme values of intravesicular $[Na^+]$ used in (*A*). All experimental boundary conditions identical to those in (*A*). All rate constants and other parameters essentially as in (*A*)

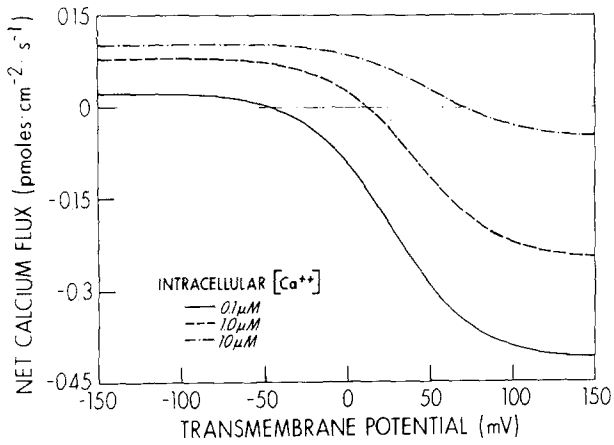

Fig. 12. Dependence of net Ca^{++} flux on transmembrane potential for the values of $[Ca^{++}]_i$ listed in the figure. Ionic parameters chosen to match those of normal intact squid axon (Requena, 1983). $[Ca^{++}]_o$ = 3 mM, $[Na^+]_o$ = 461 mM, $[Na^+]_i$ = 27 mM, T = 15°C. K_B^{Na} = 30 M^{-1}; all other rate constants and parameters as in the Table

General Considerations

Simultaneous vs. Consecutive Mechanism

Blaustein (1977) considered the choice between simultaneous and consecutive mechanisms in light of experimental data obtained from squid axon, as have other authors subsequently for the same tissue (DiPolo, 1979) and for cardiac sarcolemmal vesicles (Ledvora & Hegyvary, 1983). From these and other studies, it seems to be widely held that when activation by, e.g., Ca^{++} on one side of the membrane is independent of the concentration of, e.g., Na^+ on the other side, a simultaneous transport mechanism is generally implied (Blaustein, 1977). Likewise, if the contrary is observed a consecutive mechanism is indicated (DiPolo, 1979; Ledvora & Hegyvary, 1983). Figure 11 illustrates the fallacy of this generality. Figure 11*A* shows that SIMV11 (a simultaneous mechanism) can show exactly the behavior that would, given the above criteria, be expected of a consecutive mechanism, whereas in Fig. 11*B* behavior supposedly characteristic of a simultaneous mechanism is displayed by the consecutive mechanism, SEQV7. The same ionic boundary conditions and essentially the same set of rate constants were used for both mechanisms.

Review of the squid axon literature shows that relatively little (if any) Ca^{++}–Ca^{++} exchange occurs in the absence of Na^+. In our experience with the simultaneous and consecutive mechanisms described here, such exchange appears to be inherent in consecutive mechanisms, whereas it appears inherently impossible to induce in simultaneous mechanisms. This difference is evident from simple inspection of the respective schematic diagrams of the two mechanisms in Figs. 1 and 2. There it can be seen that with the simultaneous mechanism translocation (and hence Ca^{++}–Ca^{++} exchange) can only occur when the enzyme is occupied by *both* Ca^{++} and Na^+, whereas with the consecutive mechanism Ca^{++} translocation can occur in the absence of Na^+. This fact, in our view, is the strongest argument in favor of a simultaneous rather than a consecutive mechanism for Na^+–Ca^{++} exchange. As a corollary, we view the existence of Na^+-Na^+ exchange in

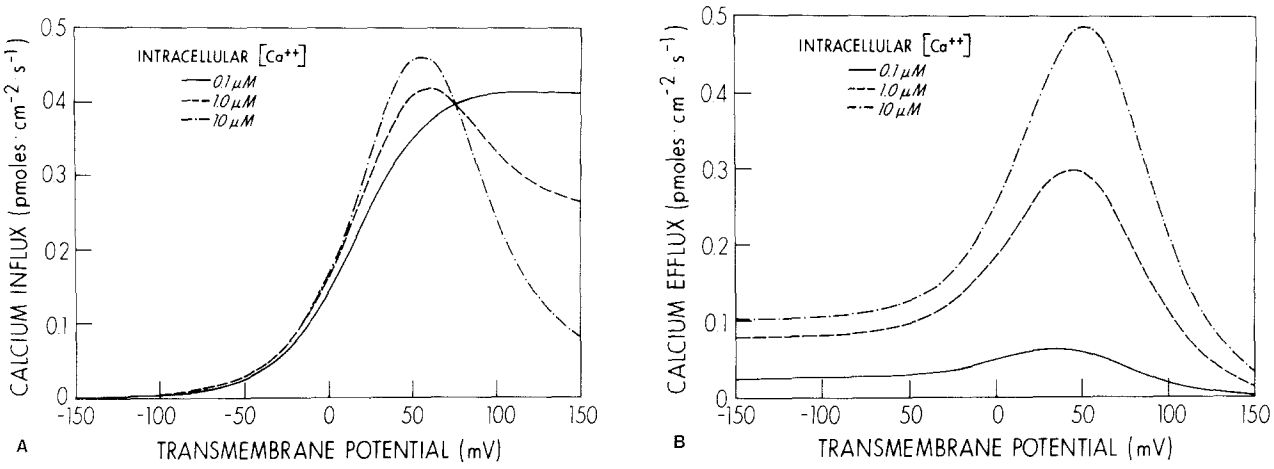

Fig. 13. Dependence of unidirectional Ca^{++} fluxes on membrane potential for the values of $[Ca^{++}]_i$ listed in the figure. (*A*) Unidirectional Ca^{++} efflux. (*B*) Unidirectional Ca^{++} influx. Ionic parameters chosen to match normal intact squid axon and are identical to those used in Fig. 12

the absence of K^+ (and *vice versa*) with the Na^+,K^+ transport pump as strong evidence for that mechanism being consecutive rather than simultaneous (Chapman et al., 1983).

Net and Unidirectional Fluxes: Effect of Transmembrane Potential

The lack of correlation between net and unidirectional ion fluxes through transport mechanisms has already been pointed out in regard to Na^+,K^+ transport (Chapman, 1982; Chapman et al., 1983). The same discrepancy is particularly evident in the behavior of the Na^+–Ca^{++} exchange mechanisms studied here. Figure 12 shows the *net* Ca^{++} flux in SIMV11 as a function of membrane potential for different values of intracellular $[Ca^{++}]$ and for boundary conditions that match those of a normal squid axon (Requena, 1983). As to be expected, the potential at which net exchange is zero (the equilibrium or reversal potential) shifts in the depolarizing direction as intracellular $[Ca^{++}]$ is raised. It should be noted that the "reversibility" of the exchanger, i.e., the magnitude of Ca^{++} influx at potentials positive to the reversal potential, is highly dependent on the intracellular concentrations of Na^+ and Ca^{++}, a finding that will be discussed in more detail in a later section concerned with excitation-contraction (EC) coupling. The behavior of the corresponding *unidirectional* Ca^{++} efflux (Fig. 13*A*) and influx (Fig. 13*B*) is dramatically at variance, however, with the net flux. Whereas the net flux is monophasic with voltage, the unidirectional Ca^{++} efflux for the ionic boundary conditions employed here is biphasic showing a maximum around 0 mV. Even more remarkable is the behavior of the unidirectional Ca^{++} influx (Fig. 13*B*) which changes from monophasic to biphasic with increase in intracellular $[Ca^{++}]$, the influx being "stimulated" at negative potentials and inhibited" at positive potentials by increasing intracellular $[Ca^{++}]$. It should be stressed, however, that these bizarre effects reflect the influence of membrane potential on Ca^{++}–Ca^{++} exchange; the net Ca^{++} flux shows a monotonic decline with depolarization under similar conditions (Fig. 10). Under experimental conditions similar to those of Allen and Baker (1983), Ca^{++}–Ca^{++} exchange through the exchanger is essentially eliminated because of the low (50 μM) external Ca^{++}, in which case unidirectional Ca^{++} efflux decreases with depolarization (*see* Fig. 7*B*) as these authors observed.

It has been presumed that the effect of membrane potential on Na^+–Ca^{++} exchange can be used to determine whether the process is electrogenic and, if so, its stoichiometry. Thermodynamically, at equilibrium the intracellular and extracellular $[Na^+]$ and $[Ca^{++}]$ must be related to the membrane potential according to Eq. (1). It cannot be emphasized too strongly, however, that the kinetic effect of a change in ion concentration or potential which disturbs such equilibrium cannot be predicted in any straightforward manner. That is to say the extent to which this equilibrium is disturbed can in no way be used to argue for a correspondingly extensive change in ion flux. This lack of correspondence between driving force and flux was vividly demonstrated in Fig. 13 where the relationship between transmembrane potential and the unidirectional Ca^{++} fluxes describes a variety of forms, unrelated to the fixed stoichiometry. Indeed, we have observed under certain conditions the unidirectional

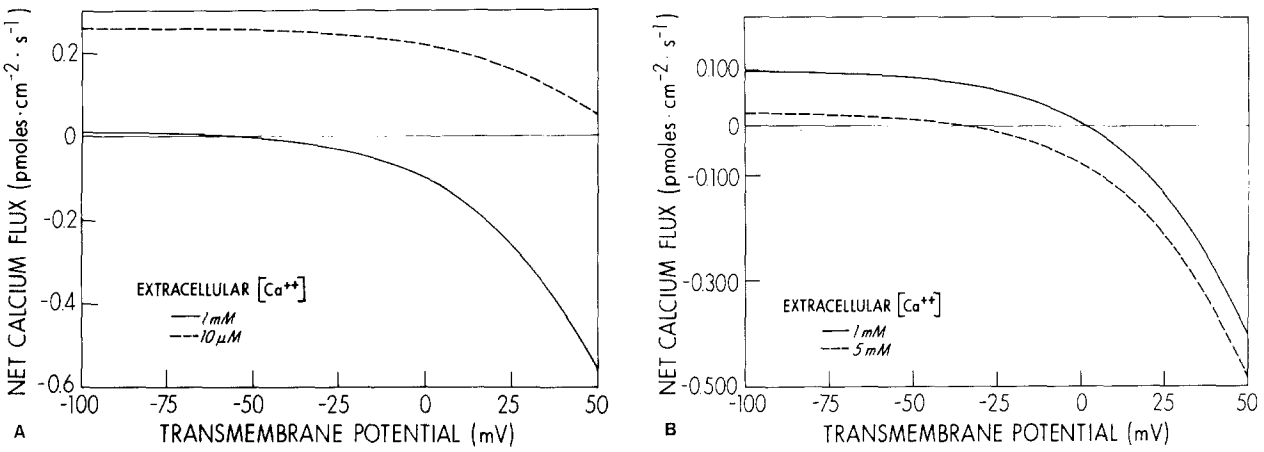

Fig. 14. Net Ca^{++} flux as a function of membrane potential for (*A*) normal (1 mM) and low (10 μM) extracellular $[Ca^{++}]$ and (*B*) for normal and high extracellular $[Ca^{++}]$. Ionic parameters chosen to match frog cardiac muscle experiments: $[Ca^{++}]_i = 0.2$ μM, $[Na^+]_o =$ 120 mM (frog Ringer's), $[Na^+]_i = 15$ mM, $T = 20$°C, $K_B^{Na} = 30$ M^{-1}, all other rate constants and parameters as in the Table

ion fluxes to be essentially independent of membrane potential. The reason for this variability is that the voltage-dependent step is more rate-limiting given some values of rate constants and boundary conditions than it is under others.

Clearly, the degree of voltage dependence of the unidirectional or net fluxes cannot be used to determine the stoichiometry of the exchange process, as has been presumed for the net fluxes (Mullins & Brinley, 1975; Mullins et al., 1983). As was demonstrated above, in the case of the unidirectional ion fluxes, the discrepancy between driving force and flux can be quite startling so that the way these fluxes change with potential has little if any value in establishing the stoichiometry of the exchange process.

Na^+–Ca^{++} Exchange and Excitation-Contraction Coupling

Na^+–Ca^{++} exchange has been identified in skeletal (Gilbert & Meissner, 1982) as well as cardiac muscle (Pitts, 1979; Reeves & Sutko, 1979) and its presence in other muscle has been implied from a variety of physiological experiments, e.g., smooth muscle (Katase & Tomita, 1972; Reuter et al., 1973). It is widely held that Na^+–Ca^{++} exchange plays a key role in excitation-contraction coupling in cardiac muscle, particularly in frog ventricular muscle where the majority if not all of the Ca^{++} activating contraction is thought to enter the cytoplasm from extracellular space. Ca^{++} is viewed as entering not only passively via a Ca^{++} channel, but also via the Na^+–Ca^{++} exchanger during the action potential when the membrane potential becomes positive to the reversal potential for the exchanger (Mullins, 1981). In mammalian heart, rather than activate contraction directly, such influx of Ca^{++} from extracellular space is thought to act as a trigger for the release (as well as determine the amount) of a second source of activator Ca^{++} located within the SR.

Dependence of Contraction on Extracellular Ca^{++}. One of the major differences between contraction of cardiac and skeletal muscle is the relative immunity of skeletal muscle contraction to the absence of extracellular Ca^{++}. In all probability this immunity is the consequence of the relatively low level of Na^+–Ca^{++} exchange activity found in skeletal muscle (40 pmol Ca^{++}/mg sarcolemmal vesicular protein/sec, Gilbert & Meissner, 1982) compared with cardiac muscle (15 to ≈30 nmol Ca^{++}/mg protein/sec, Caroni et al., 1980; Caroni & Carafoli, 1983).

As first shown by Ringer (1883), cardiac muscle, especially that of frog, is exquisitely sensitive to the extracellular $[Ca^{++}]$: contractions rapidly disappear when the muscle is exposed to Ca^{++}-free solutions. Moreover, sudden increases and decreases in extracellular $[Ca^{++}]$ during the course of a contraction produce equally sudden increases and decreases in the force of contraction (Kavaler, 1974; Einwacher & Brommundt, 1978), leading to the inescapable conclusion that contraction and relaxation of frog heart muscle is controlled by the influx and efflux, respectively, of Ca^{++} from the cell.

Figure 14*A* shows net Ca^{++} flux as a function of membrane potential for low (10 μM) and normal (1 mM) $[Ca^{++}]_o$. The resting $[Ca^{++}]_i$ was assumed to

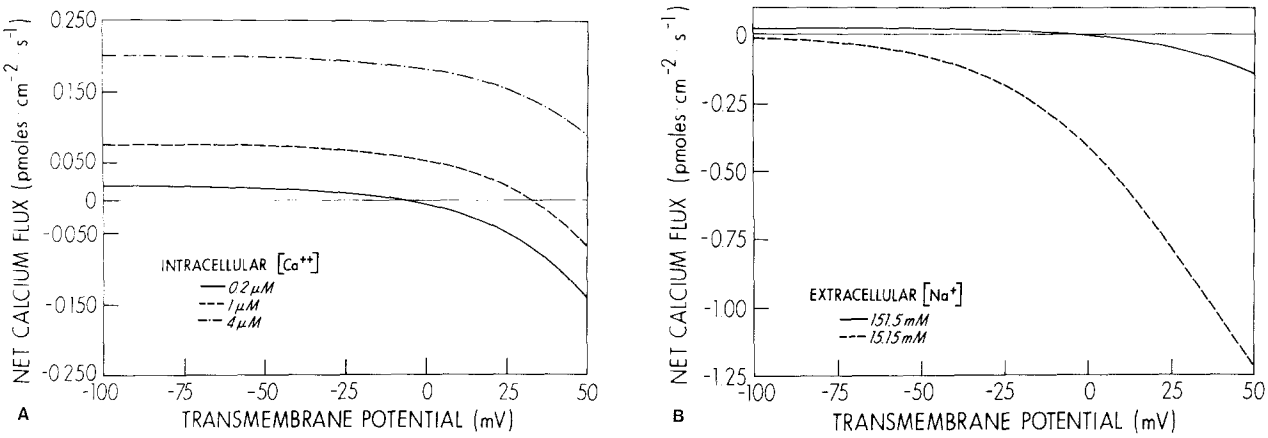

Fig. 15. Net Ca^{++} flux as a function of membrane potential for (*A*) normal (151.5 mM) $[Na^+]_o$ with the 3 values of $[Ca^{++}]_i$ listed in the figure and (*B*) normal (151.5 mM) and low (15.5 mM) $[Na^+]_o$. Ionic parameters chosen to match mammalian ventricular muscle (Sheu & Fozzard, 1982): $[Ca^{++}]_o$ = 1.8 mM, $[Na^+]_o$ = 151.5 mM, $[Na^+]_i$ = 8.4 mM. In (*B*) $[Ca^{++}]_i$ = 270 nM. T = 37°C. K_B^{Na} = 30 M^{-1}; all other rate constants and parameters as in the Table

be the same as mammalian cardiac muscle (200 nM); $[Na^+]_o$ = 120 mM (frog Ringer's) and $[Na^+]_i$ equaled the value estimated by Chapman (1983) for frog cardiac muscle. At normal $[Ca^{++}]_o$, Ca^{++} efflux is relatively small and independent of membrane potential for potentials negative to the reversal potential, illustrating again the dubious validity of arguments that are based on a presumed direct relationship between the magnitude of the flux and the driving force. When $[Ca^{++}]_o$ is reduced to 10 μM, Ca^{++} efflux is greatly increased over the entire physiological range of potentials, which could account for the loss of contractility when cardiac muscle is exposed to solutions containing nominally zero $[Ca^{++}]$. The marked activation of Ca^{++} efflux would also be in keeping with the observation that lowering $[Ca^{++}]_o$ causes a large increase in $[Na^+]_i$ (Chapman, 1983), presumably as a consequence of a correspondingly large influx of Na^+ via the Na^+–Ca^{++} exchanger—an amount sufficient to drive the Na,K pump from its normal set point.

This behavior of SIMV11 must not, however, be construed as an inevitable property of the mechanism. For example, a (mathematically) simplified version of SIMV11 (referred to in footnote [1]), using essentially the same rate constants as used here with SIMV11, showed relatively little increase in Ca^{++} efflux when the $[Ca^{++}]_o$ was reduced to 10 μM. Possibly, similar behavior could be induced in SIMV11 by an appropriate change in rate constants.

Nonetheless, whether the Ca^{++} efflux induced by the low $[Ca^{++}]_o$ is large or small, a second immediate effect of the low $[Ca^{++}]_o$ would be inescapable, namely the influx of Ca^{++} that normally would have occurred during the action potential, i.e., as the membrane potential executed its trajectory to the right along the voltage axis of Fig. 15*A*, would be abolished.

The more immediate effect of an *increase* in extracellular $[Ca^{++}]$ during the time-course of a contraction (Kavaler, 1974) is simulated in Fig. 14*B* where for the normal $[Ca^{++}]_o$ curve, $[Ca^{++}]_i$ is assumed to have increased from its resting value of 0.27 μM (*cf.* corresponding curve in Fig. 17*A*) to 2.0 μM (Fabiato, 1981). As can be seen by comparing the curves of Fig. 14*A* and *B* for 1 mM $[Ca^{++}]_o$, this rise in $[Ca^{++}]_i$ greatly reduces the influx of Ca^{++} which, as shown in Fig. 14*B*, is largely restored by the increase in $[Ca^{++}]_o$.

The results of Einwacher and Brommundt (1978) are particularly relevant to the above findings. Their experimental records show that during contractures induced by depolarizing voltage-clamp pulses, the outward membrane current required to maintain the steady depolarization *increased* when the extracellular $[Ca^{++}]$ was suddenly increased (or the extracellular $[Na^+]$ was decreased) to cause a sudden increase in the force of the contraction. The direction of the change in membrane current produced by the increase in Ca^{++} was opposite to that expected were the Ca^{++} to have entered by a Ca^{++}-permeable channel, but was in the direction expected if the entry was via an electrogenic Na^+–Ca^{++} mechanism of the kind studied here. The similarity in effect of a drop in extracellular $[Na^+]$ to an increase in $[Ca^{++}]$ (and *vice versa*) further supports this conclusion. The observed change in membrane current cannot be unequivocally interpreted as evidence for the electrogenicity of Na^+–Ca^{++} exchange, however, since the changes in intracellular $[Ca^{++}]$ produced by fluxes through the Na^+–Ca^{++} exchanger could be said to have activated a Ca^{++}-

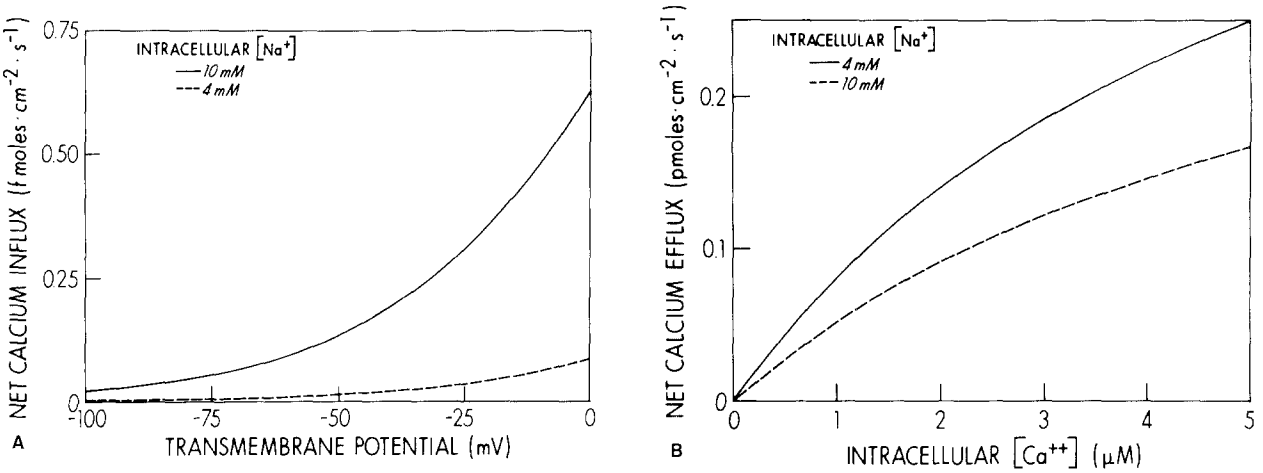

Fig. 16. (*A*) The dependence of net Ca^{++} influx on transmembrane potential at reduced (14 mM) $[Na^+]_o$, for normal (10 mM) and reduced (4 mM) $[Na^+]_i$, matching the experiments of Ellis (1977) with sheep cardiac Purkinje fibers: $[Ca^{++}]_o$ = 2 mM, $[Ca^{++}]_i$ = 0.27 μM. (*B*) Dependence of net Ca^{++} efflux on $[Ca^{++}]_i$ at normal (140 mM) $[Na^+]_o$ for normal and reduced $[Na^+]_i$. Transmembrane potential = −90 mV; T = 37°C. In both (*A*) and (*B*), K_B^{Na} = 30 M^{-1}; all other rate constants and parameters as in the Table

activated K^+ permeability mechanism, of the kind first described by Meech and Strumwasser (1970), thereby causing the observed increase in outward membrane current.

The factors governing intracellular $[Ca^{++}]$ are complex and are not readily investigated by the static studies that are the main concern of the present paper. The factors become especially complex when the sources of cytoplasmic Ca^{++} include intracellular stores such as the SR. As can be seen from Fig. 14*A*, the rate of Ca^{++} efflux via the Na^+–Ca^{++} exchanger is dramatically increased at the resting potential when $[Ca^{++}]_i$ increases, the highest value for $[Ca^{++}]_i$ being that estimated to occur physiologically (≈4 μM, Fabiato, 1981). At moderately elevated $[Ca^{++}]_i$, the effect of membrane depolarization is to inhibit Ca^{++} efflux, influx being greatly reduced once $[Ca^{++}]_i$ increases appreciably above the resting value. This inhibition of Ca^{++} efflux will be especially important in those hearts where a significantly large fraction of activating Ca^{++} comes from the SR, for as can be seen from Fig. 15*A*, more of this Ca^{++} could be extruded from the cell by the activated Na^+–Ca^{++} exchanger if the membrane potential returned to its resting value. A full understanding and appreciation of the interaction of changing action potential time-course, intracellular $[Ca^{++}]$ and $[Na^+]$, with the kinetics of Ca^{++}-binding to the contractile proteins and uptake and release from the SR (Robertson et al., 1982; Gillis et al., 1982), must await the results of planned studies of the kinetics of the intracellular $[Ca^{++}]$-regulating system.

Low Sodium Contractures. When exposed to bathing solutions low in Na^+, resting cardiac muscle undergoes a contracture that slowly relaxes with time. In general these contractures have been accounted for in terms of Na^{++}-Ca^{++} exchange. As pointed out above (*cf.* Figs. 10 and 12), the "reversibility" of Na^+–Ca^{++} exchange (i.e., its ability to transport Ca^{++} into the cell in exchange for intracellular Na^+) is highly dependent on the ionic boundary conditions as well as the transmembrane potential. For ionic conditions similar to those found in cardiac muscle, the reversibility is markedly enhanced by reducing the extracellular $[Na^+]$. Figure 15*B* shows the effect of a tenfold reduction in extracellular $[Na^+]$. At normal $[Na^+]_o$ there is a net efflux of Ca^{++} that is independent of membrane potential in the negative range, which is transformed into a net influx at the lower $[Na^+]_o$ that now varies substantially over the same range of potentials, although it is virtually unaffected by the consequent rising $[Ca^{++}]_i$ (*not shown*). In the experiments of Ellis (1977) with sheep Purkinje fibers, when $[Na^+]_o$ was reduced tenfold (the electrochemical gradient for Na^+ remaining inward), Ellis observed a decline in $[Na^+]_i$ (from 10 mM in his experiments) to a steady value of ≈4 mM. As can be seen from Fig. 16*A*, the Ca^{++} influx (Na^+ efflux) at low $[Na^+]_o$ is dramatically inhibited by the decline in $[Na^+]_i$ from 10 to 4 mM. Undoubtedly, it is such fall in $[Na^+]_i$ that causes the contracture to disappear eventually (as observed experimentally), $[Na^+]_i$ settling down to a new steady value as the Ca^{++} influx becomes sufficiently small to be extruded via the sarcolemmal ATP-driven Ca^{++} pump (Caroni & Carafoli, 1981). On the other hand, on returning to 140 mM $[Na^+]_o$—after the decline in $[Na^+]_i$—the factors influencing the consequent Ca^{++} efflux (Na^+ influx) are quite different. As can be seen from Fig. 16*B*,

the resulting Ca^{++} efflux (Na^+ influx) via the exchanger is relatively little affected by the consequent rise in $[Na^+]_i$, but the accompanying decline in $[Ca^{++}]_i$ dramatically inhibits the efflux.

As can be seen from Fig. 15*B*, the rate of Ca^{++} influx at depolarized potentials is enhanced by a reduction in extracellular $[Na^+]$. This would readily explain the finding that if the fiber is maintained in the low Na^+ medium until the contracture relaxes, it will respond with a second contracture if depolarized by immersion in high K^+-containing solutions. This same figure also shows why a small reduction in extracellular $[Na^+]$, insufficient to cause a detectable contracture, would have a positive inotropic action. Although the reduction would produce an insignificant change in resting Ca^{++} efflux by the exchanger, it would enhance the influx that occurs during depolarization associated with an action potential.

The Positive Inotropic Effect of Cardiac Glycosides. The positive inotropic effect of cardiac glycosides has been thought to be linked to an effect on Na^+–Ca^{++} exchange through the increase in intracellular $[Na^+]$ brought about by the drug's inhibition of sarcolemmal Na^+,K^+ transport. Although small changes in intracellular $[Na^+]$ could produce proportionately larger changes in intercellular $[Ca^{++}]$, the equilibrium value for intracellular $[Ca^{++}]$ in normal cardiac muscle (e.g., $[Na^+]_o$ = 140 mM, $[Na^+]_i$ = 10 mM, $[Ca^{++}]_o$ = 1 mM V_m = −85 mV and a stoichiometry of 3 Na^+ to 1 Ca^{++}) is so low (15 nM) that even for an increase of $[Na^+]_i$ from 10 to 15 mM, the resultant equilibrium value for $[Ca^{++}]_i$ (50 nM) is still well below the resting value, never mind the threshold value for activation of contraction. It is therefore not clear how such an increase in $[Na^+]_i$ could lead to an increased force of contraction. In the same way, as argued by Mullins (1984), it is difficult to account (primarily in terms of Na^+–Ca^{++} exchange) for the finding of Eisner et al. (1981) that increases in $[Na^+]_i$ which had negligible effect on the resting tension of sheep cardiac Purkinje fibers were associated with striking increases in developed tension during contractions. The results obtained from SIMV11 shown in Fig. 17 suggest a possible mechanism. In this figure, net Ca^{++} flux is plotted as a function of membrane potential for the range of $[Na^+]_i$ (8 to 16 mM) found in the experiments of Eisner et al. (1981). These increases in $[Na^+]_i$ produce relatively insignificant reductions in resting Ca^{++} efflux, which could readily be balanced by increased activity of the sarcolemmal Ca^{++} pump, especially in view of its relatively low K_m for Ca_i^{++} of ≈0.2 μM (Caroni & Carafoli, 1981). As a consequence little or no change in $[Ca^{++}]_i$ would result and hence negligible change in resting

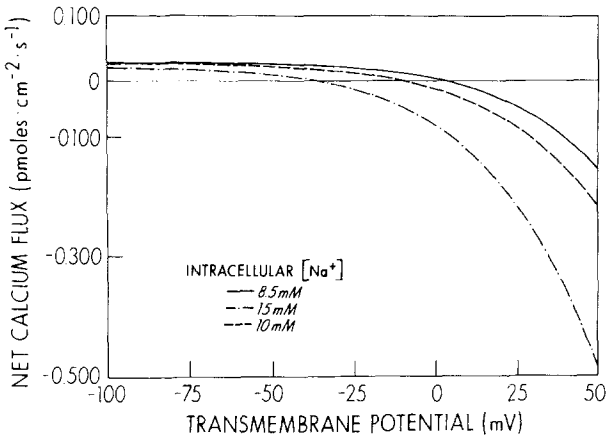

Fig. 17. Dependence of net Ca^{++} flux on transmembrane potential for normal (8.4 mM) and two elevated values of $[Na^+]_i$ (listed in the figure) that might be caused by cardiac-glycoside inhibition of sarcolemmal Na,K transport. Ionic parameters chosen to match the average values found for resting cardiac ventricular muscle (Sheu & Fozzard, 1982): $[Na^+]_o$ = 151.5 mM, $[Ca^{++}]_o$ = 1.8 mM, $[Ca^{++}]_i$ = 0.27 μM, T = 37°C. K_B^{Na} = 30 M^{-1}, all other rate constants and parameters as in the Table

tension. On the other hand, the influx of Ca^{++} that results from depolarization and reversal of Na^+–Ca^{++} exchange is greatly increased by an increase in $[Na^+]_i$. Even an increase in $[Na^+]_i$ as small as 1 mM produces a sizeable increment in the rate of Ca^{++} influx at depolarized potentials which, integrated over the time-course of potential change associated with an action potential, could account for the positive inotropic effect of cardiac glycosides that produce correspondingly small increments in $[Na^+]_i$.

We wish to thank Dr. J.B. Chapman for his participation in the early stages of this work. The work was supported in part by USPHS grants RR-01693 and HL-12157 and a grant from the Kemshall Fund.

References

Allen, D.G., Baker, P.F. 1983. Comparison of the effects of potassium and electrical depolarization on Na–Ca exchange in squid axons. *J. Physiol. (London)* **345:**80P

Baker, P.F. 1972. Transport and metabolism of calcium ions in nerve. *Prog. Biophys. Mol. Biol.* **24:**177–223

Baker, P.F. 1976. *In:* Calcium in Biological Systems. *Symp. Soc. Exp. Biol.* p. 70

Baker, P.F., Blaustein, M.P., Hodgkin, A.L, Steinhardt, R.A. 1967. The effect of sodium concentration on calcium movements in giant axons of *Loligo forbesi*. *J. Physiol. (London)* **192:**43P–44P

Baker, P.F., Blaustein, M.P., Hodgkin, A.L, Steinhardt, R.A. 1969. The influence of calcium on sodium efflux in squid axons. *J. Physiol. (London)* **200:**431–458

Baker, P.F., Hodgkin, A.L., Ridgway, E.B. 1971. Depolarization and calcium entry in squid giant axons. *J. Physiol. (London)* **218:**709–755

Baker, P.F., McNaughton, P.A. 1976*a*. Kinetics and energetics of calcium efflux from intact squid giant axons. *J. Physiol. (London)* **259:**103–144

Baker, P.F., McNaughton, P.A. 1976*b*. The effect of membrane potential on the calcium transport systems in squid axons. *J. Physiol. (London)* **260:**24P

Baker, P.F., McNaughton, P.A. 1978. The influence of extracellular calcium binding on the calcium efflux from squid axons. *J. Physiol. (London)* **276:**127–150

Bers, D.M., Philipson, K.D., Nishimoto, A.Y. 1980. Sodium-calcium exchange and sidedness of isolated cardiac sarcolemmal vesicles. *Biochim. Biophys. Acta* **601:**358–371

Blaustein, M.P. 1977. Effects of internal and external cations and of ATP on sodium-calcium and calcium-calcium exchange in squid axons. *Biophys. J.* **20:**79–111

Blaustein, M.P., Russell, J.M. 1975. Sodium-calcium exchange and calcium-calcium exchange in internally dialyzed squid giant axons. *J. Membrane Biol.* **22:**285–312

Blaustein, M.P., Russell, J.M., De Weer, P. 1974. Calcium efflux from internally dialyzed squid axons: The influence of external and internal cations. *J. Supramol. Struct.* **2:**558–581

Bridge, J.H.B., Bassingthwaighte, J.B. 1983. Uphill sodium driven by an inward calcium gradient in heart muscle. *Science* **219:** 178–179

Brinley, F.J., Jr., Spangler, S.G., Mullins, L.J. 1975. Calcium and EDTA fluxes in dialyzed squid axons. *J. Gen. Physiol.* **66:**223–250

Caroni, P., Carafoli, E. 1981. The Ca^{++}-pumping ATPase of heart sarcolemma. *J. Biol. Chem.* **256:**3263–3270

Caroni, P., Carafoli, E. 1983. The regulation of the Na^+–Ca^{++} exchanger of heart sarcolemma. *Eur. J. Biochem.* **132:**451–460

Caroni, P., Reinlib, L., Carafoli, E. 1980. Charge movements during the Na^+–Ca^{++} exchange in heart sarcolemmal vesicles. *Proc. Natl. Acad. Sci. USA* **77:**6354–6358

Chapman, J.B. 1982. A kinetic interpretation of "variable" stoichiometry for an electrogenic sodium pump obeying chemiosmotic principles. *J. Theor. Biol.* **95:**665–678

Chapman, J.B., Johnson, E.A., Kootsey, J.M. 1983. Electrical and biochemical properties of an enzyme model of the sodium pump. *J. Membrane Biol.* **74:**139–153

Chapman, R.A. 1983. Control of cardiac contractility at the cellular level. *Am. J. Physiol.* **245:**H535–H552

Daut, J., Rudel, R. 1981. Cardiac glycoside binding to the Na/K-ATPase in the intact myocardial cell: Electrophysiological measurement of chemical kinetics. *J. Mol. Cell. Cardiol.* **13:**777–782

DiPolo, R. 1973. Calcium efflux from internally dialyzed squid giant axons. *J. Gen. Physiol.* **62:**575–589

DiPolo, R. 1979. Calcium influx in internally dialyzed squid giant axons. *J. Gen. Physiol.* **73:**91–113

DiPolo, R., Beauge, L. 1979. Physiological role of ATP-driven calcium pump in squid axon. *Nature (London)* **278:**271–273

DiPolo, R., Beauge, L. 1980. Mechanisms of calcium transport in the giant axon of the squid and their physiological role. *Cell Calcium* **1:**147–169

DiPolo, R., Beauge, L. 1981. The effects of vanadate on calcium transport in dialyzed squid axons. Sidedness of vanadate-cation interactions. *Biochim. Biophys. Acta* **645:**229–236

DiPolo, R., Beauge, L. 1983. The calcium pump and sodium-calcium exchange in squid axons. *Annu. Rev. Physiol.* **45:**313–324

DiPolo, R., Rojas, H., Vergara, J., Lopez, R., Caputo, C. 1983. Measurements of intracellular ionized calcium in squid giant axons using calcium-selective electrodes. *Biochim. Biophys. Acta* **728:**311–318

Einwachter, H.M., Brommundt, G. 1978. Transient tension responses of voltage-clamped frog atrial muscle related to sudden changes in external Ca or Na. *Pfluegers Arch.* **375:**69–73

Eisner, D.A., Lederer, W.J., Vaughan-Jones, R.D. 1981. The dependence of sodium pumping and tension on intracellular sodium activity in voltage-clamped sheep Purkinje fibres. *J. Physiol. (London)* **317:**163–187

Ellis, D. 1977. The effects of external cations and ouabain on the intracellular sodium activity of sheep heart Purkinje fibres. *J. Physiol. (London)* **273:**211–240

Fabiato, A. 1981. Myoplasmic free calcium concentration reached during the twitch of an intact isolated cardiac cell and during calcium-induced release of calcium from the sarcoplasmic reticulum of a skinned cardiac cell from the adult rat or rabbit ventricle. *J. Gen. Physiol.* **78:**457–497

Gilbert, J.R., Meissner, G. 1982. Sodium-calcium ion exchange in skeletal muscle sarcolemmal vesicles. *J. Membrane Biol.* **69:**77–84

Gillis, J.M., Thomason, D., Lefevre, J., Kretsinger, R.H. 1982. Parvalbumins and muscle relaxation: A computer simulation study. *J. Muscle Res. Cell Motility* **3:**377–398

Holt, D.C., Kootsey, J.M. 1984. SCoP: A simulation control program for mini/microcomputers. National Biomedical Simulation Resource, Duke University Medical Center, Durham, N.C.

Jencks, W.P. 1982. Rules and the economics of energy balance in coupled vectorial processes. *In:* Membranes and Transport: A Critical Review. A. Martinosi, editor. pp. 510–520. Plenum, New York

Johnson, E.A., Chapman, J.B. 1985. A working mechanism of the Na,K-pump: Ion binding. *In:* The Company of Biologists. *(in press)*

Katase, T., Tomita, T. 1972. Influences of sodium efflux and calcium on the recovery process from potassium contracture in the guinea-pig taenia coli. *J. Physiol. (London)* **224:**489–500

Kavaler, F. 1974. Electrochemical time course in frog ventricle manipulation of calcium level during voltage clamp. *J. Mol. Cell. Cardiol.* **6:**575–580

Kernighan, B.W., Ritchie, D.M. 1978. The C Programming Language. Bell Telephone Laboratories, Inc., Prentice-Hall, Englewood Cliffs, N.J.

Ledvora, R.F., Hegyvary, C. 1983. Dependence of Na^+–Ca^{++} exchange and Ca^{++}–Ca^{++} exchange on monovalent cations. *Biochim. Biophys. Acta* **729:**123–136

Meech, R.W., Strumwasser, F. 1970. Intracellular calcium injection activates potassium conductance in *Aplysia* nerve cells. *Proc. Fed. Am. Soc. Exp. Biol.* **29:**834

Michael, L.H., Schwartz, A., Wallick, E.T. 1979. Nature of the transport adenosine triphosphatase-digitalis complex: XIV. Inotropy and cardiac glycoside interaction with cat ventricular muscle. *Mol. Pharmacol.* **16:**135–146

Mullins, L.J. 1977. A Mechanism for Na/Ca transport. *J. Gen. Physiol.* **70:**681–695

Mullins, L.J. 1981. Ion Transport in Heart. Raven, New York

Mullins, L.J. 1984. An electrogenic saga: Consequences of sodium-calcium exchange in cardiac muscle. *In:* Electrogenic Transport: Fundamental Principles and Physiological Implications. M.P. Blaustein and M. Lieberman, editors. Raven, New York

Mullins, L.J., Brinley, F.J., Jr. 1975. Sensitivity of calcium ef-

flux from squid axons to changes in membrane potential. *J. Gen. Physiol.* **65:**135–152

Mullins, L.J., Tiffert, T., Vassort, G., Whittembury, J. 1983. Effects of internal sodium and hydrogen ions and of external calcium ions and membrane potential on calcium entry in squid axons. *J. Physiol. (London)* **338:**295–319

Philipson, K.D., Nishimoto, A.Y. 1981. Efflux of Ca^{++} from cardiac sarcolemmal vesicles. Influence of external Ca^{++} and Na^+. *J. Biol. Chem.* **256:**3698–3702

Philipson, K.D., Nishimoto, A.Y. 1982. Na^+–Ca^{++} exchange in inside-out cardiac sarcolemmal vesicles. *J. Biol. Chem.* **257:**5111–5117

Pitts, B.J.R. 1979. Stoichiometry of sodium-calcium exchange in cardiac sarcolemmal vesicles. *J. Biol. Chem.* **254:**6232–6235

Reeves, J.P., Sutko, J.L. 1979. Sodium-calcium ion exchange in cardiac sarcolemmal vesicles. *Proc. Natl. Acad. Sci. USA* **76:**590–594

Reeves, J.P., Sutko, J.L. 1983. Competitive interactions of sodium and calcium with the sodium-calcium exchange system of cardiac sarcolemmal vesicles. *J. Biol. Chem.* **258:**3178–3182

Requena, J. 1978. Calcium efflux from squid axons under constant electrochemical gradient. *J. Gen. Physiol.* **72:**443–470

Requena, J., Mullins, L.J. 1979. Calcium movement in nerve fibres. *Q. Rev. Biophys.* **12:**371–460

Requena, J. 1983. Calcium transport and regulation in nerve fibers. *Annu. Rev. Biophys. Bioeng.* **12:**237–257

Reuter, H., Blaustein, M.P., Haeusler, G. 1973. Na–Ca exchange and tension development in arterial smooth muscle. *Philos. Trans. R. Soc. London B* **265:**87–94

Ringer, S. 1883. A further contribution regarding the influence of the different constituents of the blood on the contraction of the heart. *J. Physiol. (London)* **4:**29–42

Robertson, S.P., Johnson, J.D., Potter, J.D. 1982. The time-course of Ca^{++} exchange with calmodulin, troponin, parvalbumin, and myosin in response to transient increases in Ca^{++}. *Biophys. J.* **34:**559–569

Sanders, D., Hansen, U.-P., Gradmann, D., Slayman, C.L. 1984. Generalized kinetic analysis of ion-driven cotransport systems: A unified interpretation of selective ionic effects on Michaelis parameters. *J. Membrane Biol.* **77:**123–152

Sheu, S.-S., Fozzard, H.A. 1982. Transmembrane Na^+ and Ca^{++} electrochemical gradients in cardiac muscle and their relationship to force development. *J. Gen. Physiol.* **80:**325–351

Slaughter, R.S., Sutko, J.L., Reeves, J.P. 1983. Equilibrium calcium-calcium exchange in cardiac sarcolemmal vesicles. *J. Biol. Chem.* **258:**3183–3190

Venosa, R.A., Horowicz, P. 1981. Density and apparent location of the sodium pump in frog sartorius muscle. *J. Membrane Biol.* **59:**225–232

Wong, A.Y.K., Bassingthwaighte, J.B. 1981. The kinetics of Ca-Na exchange in excitable tissue. *Math. Biosci.* **53:**275–310

Received 10 December 1984; revised 21 March 1985